AFCRL-1022

Scientific Report Number 5

AN UPWARD PULSE DELAY SYSTEM FOR MEASURING ELECTRON DENSITIES OF THE IONOSPHERE

UNIVERSITY OF UTAH

UPPER AIR RESEARCH LABORATORY

SALT LAKE CITY, UTAH

The research reported in this document has been sponsored by the Geophysics Research Directorate, Air Force Cambridge Research Laboratories, Office of Aerospace Research, United States Air Force.

(18) (19) AFCRL - 1022

(14) Scientific Report No. 5

(4) # 8,110

(5) 906500

(6) AN UPWARD PULSE DELAY SYSTEM FOR MEASURING ELECTRON DENSITIES OF THE IONOSPHERE

(7) NA

(8) NA

(10) I.

Compiled By

Robert E. Watson •

(11) 1961.

(12) 81p.

(13) NA

University of Utah
Upper Air Research Laboratory
Salt Lake City, Utah

(9) Final Report under (15) Contract No. AF-19(604)-2227

The research reported in this document has been sponsored by the Air Force Cambridge Research Laboratories, Office of Aerospace Research, United States Air Force, Bedford, Massachusetts.

(16-17) NA

(20) U.

(21) NA

Submitted By:

Obed C. Haycock 19 Dec. 1961

Obed C. Haycock — Date
Chief Investigator

AFCRL - 1022

Scientific Report No. 5

AN UPWARD PULSE DELAY SYSTEM FOR MEASURING ELECTRON DENSITIES OF THE IONOSPHERE

Compiled By

Robert E. Watson

University of Utah
Upper Air Research Laboratory
Salt Lake City, Utah

Final Report under Contract No. AF-19(604)-2227

The research reported in this document has been sponsored by the Air Force Cambridge Research Laboratories, Office of Aerospace Research, United States Air Force, Bedford, Massachusetts.

Submitted By:

Obed C. Haycock 19 Dec. 1961

Obed C. Haycock — Date
Chief Investigator

ERRATUM SHEET

	Page	
1.	10	Fig. 3. line missing - top C_3 to top R_s.
2.	22	Paragraph B. 1st sentence . . low frequency receiving antenna must . . . . .
3.	23	Fig. 3H Caption - Schematic Diagram of Low Frequency Receiver.
4.	31	End of 10th line, 2000 μs instead of 200 μs.
5.	43	Change .1μf decoupling cap to 5 μf, Fig. 16.
6.	49	Fig. 19. Change all 11.9 μh inductors to 23.8 μh.
7.	50	Fig. 20. Change three 2 μh inductors to 4 μh.
8.	51	Fig. 21. Change inductors in delay lines to correspond to modifications in Figs. 19 and 20.
9.	61	Add ($L/_2$) input inductor to delay line.

PREFACE

The work reported in this paper represents the composite effort of a number of men with Mr. Robert E. Watson serving as coordinator and assuming the principle responsibility of the development. Mr. Kay D. Baker also contributed much to the project. The Solid State Receiver developed for this project is primarily the work of Professor Charles Alley. Mr. John Evans and Sheil Sung carried out a large portion of the construction work.

At the time of this writing, the equipment is in essential readiness to be flown in a rocket for measuring the electron densities of the ionosphere. It is comtemplated that this rocket flight will take place early in the year 1962.

ABSTRACT

A system is described which measures the free electron content of the Ionosphere by the transmission of rf pulses between a rocket, which is passing through the Ionosphere, and the ground. The basic requirements and operation of the system as a whole are examined. The development and design of each of the component parts of the system are then discussed, including circuit diagrams and any important construction details. Special emphasis is placed on the design of a ground based low frequency pulsed transmitter. The transmitter was designed to operate from 4 mc to 12 mc with very little re-tuning, producing a pulse power of 20 K.W. Special provisions make it possible for the transmitter to operate at a single crystal controlled frequency or to produce a pulse train which is composed of a sequence of frequencies covering a one megacycle band. This frequency stepping feature makes it possible to examine the Ionosphere's effect on pulse propagation at several frequencies concurrently during a rocket flight. The design of a low frequency rocket-borne receiver also capable of operation from 4 mc to 12 mc is discussed in detail. The receiver is completely transistorized and incorporates a unique gated AGC system which greatly improves the signal to noise ratio in the receiver output. A ground station for receiving and recording the pulses transmitted from the rocket is also described including the circuit design of the various units.

TABLE OF CONTENTS

I. INTRODUCTION

This paper describes the development and operation of a system to be used by the Upper Air Research Laboratory at the University of Utah for conducting ionospheric research. The Upper Air Research Laboratory is at present under contract to the Air Force Cambridge Research Laboratories, Air Force Research Division to conduct experiments for measuring the free electron density in the ionosphere. One method of obtaining this data involves the transmission of radio frequency signals between a rocket which is passing through the ionized medium and the ground. A simplified analysis of the propagation characteristics of an electromagnetic wave in an ionized medium is included in Appendix I. The result of this derivation shows that if the medium is assumed lossless and the effect of the earth's magnetic field is neglected, the phase velocity of an electromagnetic wave is:

$$v_p = \frac{c}{\left[1 - \left(f_c/f\right)^2\right]^{1/2}} \qquad (1)$$

$c = 3 \times 10^8$ meters/sec

f_c = plasma frequency

f = freq. of the E.M. wave

and the group velocity is:

$$v_g = c\left[1 - \left(f_c/f\right)^2\right]^{1/2} \qquad (2)$$

These expressions will be recognized as the familiar waveguide equations except the term f_c is here re-defined as a quantity called the plasma frequency of the ionized medium. The physical significance of the f_c is that below this frequency the effective dielectric constant becomes negative and the propagation constant is imaginary.

$$f_c = \frac{\omega_c}{2\pi} = \frac{1}{2\pi}\left[\frac{Ne^2}{\epsilon_o M_e}\right]^{1/2} \qquad (3)$$

N = electron density in $^{elect}/_{m^3}$
e = electron charge 1.6×10^{-19} cou.
ϵ_o = perm. free space = 8.85^{-12} $\frac{farads}{m}$
M_e = Mass of electron = 9.1×10^{-31} kg.

Two basic methods of obtaining the electron density (N) now are readily apparent. Measurement of either the group or phase velocity of a wave propagating through the ionized medium will be sufficient to determine N. Both of these methods and others have in fact been used with good success.[1,2] Using the method of transmission of radio frequency signals between a rocket in the ionosphere and the earth, it is not possible to measure directly either of these quantities instantaneously at any point in the propagation path. The basic measurement must therefore be a comparison between two signals. The frequency of one signal is relatively near the plasma frequency of the medium such that it experiences group and phase velocities different than c and, the other signal has a frequency which

---

[1] D.J. Baker "Electron Densities of the Ionosphere Utilizing High Altitude Rockets", Ph.D. Thesis Elect. Eng., Univ. of Utah, 1956.

[2] J.E. Jackson, "Measurement of the E-layer with the Navy Viking Rocket," J. Geophys. Res., Vol. 59, P. 377; 1954.

is high compared to the plasma frequency such that it is essentially unaffected by the ionosphere.

This paper describes a system which measures the relative decrease in group velocity of a radio frequency pulse which passes through the ionosphere. This involves the transmission of two signals through the ionosphere from ground based transmitters to rocketborne receivers. One signal is a UHF reference pulse which is negligibly affected by passage through the ionized medium; and the other is a probing frequency pulse which is slightly above the plasma frequencies of the ionospheric layers to be penetrated. The relative transit time of the two signals through the ionosphere is determined by telemetering their arrival times at the rocket back to ground receiving and recording stations. The relative increase in transit time of the probing frequency pulse compared to the reference pulse is a measure of the group velocity of the low frequency pulse if the rocket position is known so that the propagation path is determined. From this information, the electron density can then be determined.[3]

The primary problem encountered by the author was the design and construction of the probing frequency transmitter. This paper will therefore discuss the system as a whole and the function of each of the individual components without great detail, and then present more specifically the design details of the transmitter. The basic requirements of the low frequency transmitter are given in Table I. Note that the

---

[3]Baker, op. cit., p. 30-37

operating frequency must be variable from 4 to 12 mc with an overall bandwidth of one mc or greater. This requirement presents some unique problems if the operating frequency is to be readily adjustable over this entire range with a minimum of involved re-tuning procedures. Another unusual design feature of the transmitter is the provision for stepping frequencies over any one mc band within the range of operating frequencies. This feature makes it possible to obtain a family of curves of electron density vs. altitude for several frequencies within any one mc band.

TABLE I.

Transmitter Specifications

1. Center frequency - 4 to 12 mc.
2. Modulation - 5 μs pulse with p.r.f. of approx. 200 cycles/sec.
3. Power - 20 kw peak pulse.
4. Step frequency - the transmitter must be capable of stepping frequencies over a one mc band at any center frequency within the operating range, the number of steps being adjustable with proper coding to indicate the beginning of each stepping sequence.
5. Single freq. crystal control - when stepping over a band of frequencies is not desirable, it must be possible to operate at a single crystal controlled frequency.
6. Size - The entire unit must be physically small and light enough to be readily portable.

II. SYSTEM REQUIREMENTS

The complete system for measuring the electron density of the ionospheric layers by pulse propagation delay methods is shown in block form in Fig. 1. Basically, it consists of two ground based transmitters which transmit pulses with a given time synchronization, their respective airborne receivers, a high frequency telemetry system for relaying the time of arrival information of the two upward pulses back to the earth, and a recording station to continuously record this information during the experiment. Reduction of the pulse delay data to yield electron density information requires in addition that the rocket position also be accurately determined. This information is supplied by an s-band radar unit with the aid of a transponder located in the rocket. The complete timing sequence of events both on the ground and in the rocket is shown in graphic form in Fig. 2.

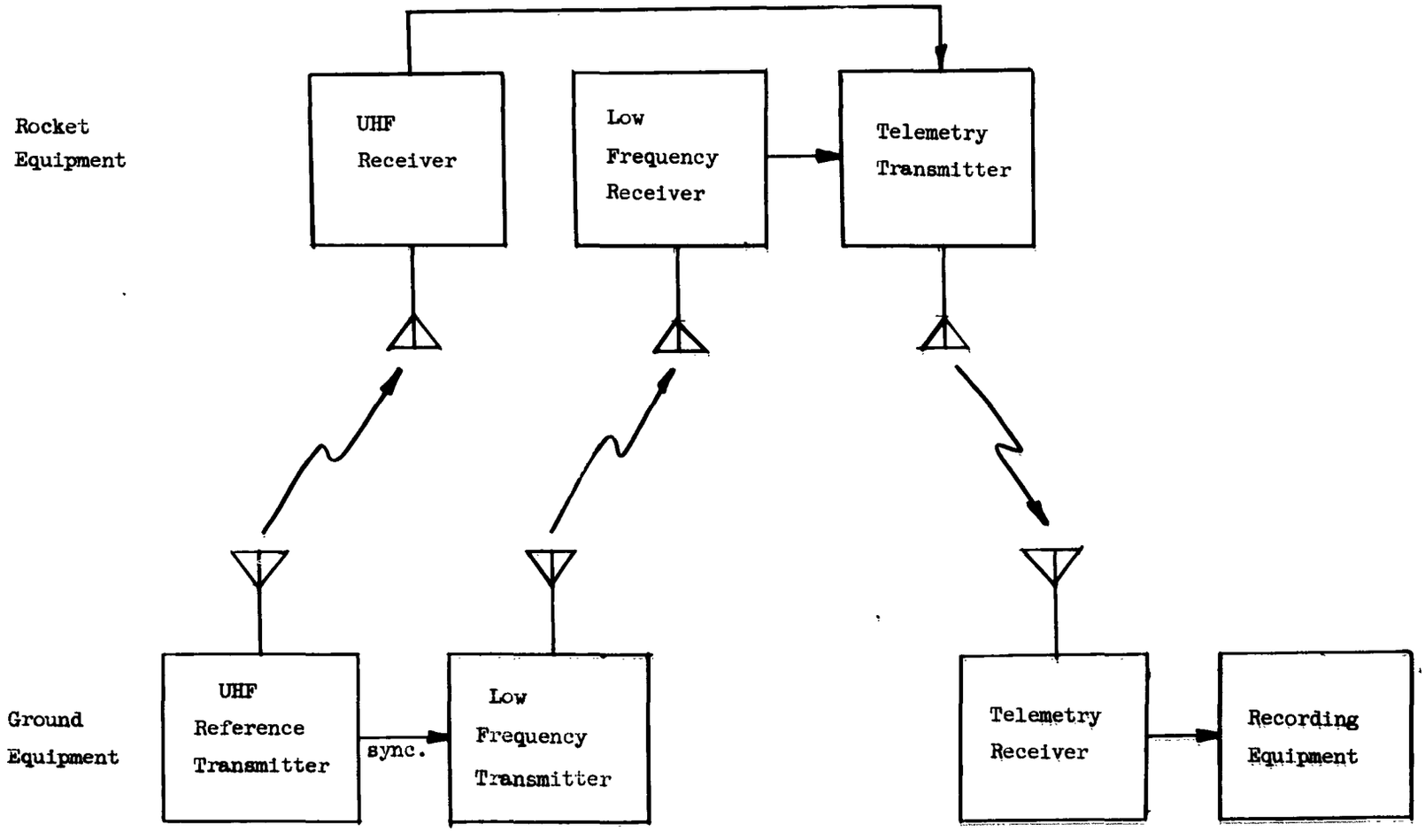

Figure 1. SYSTEM BLOCK DIAGRAM

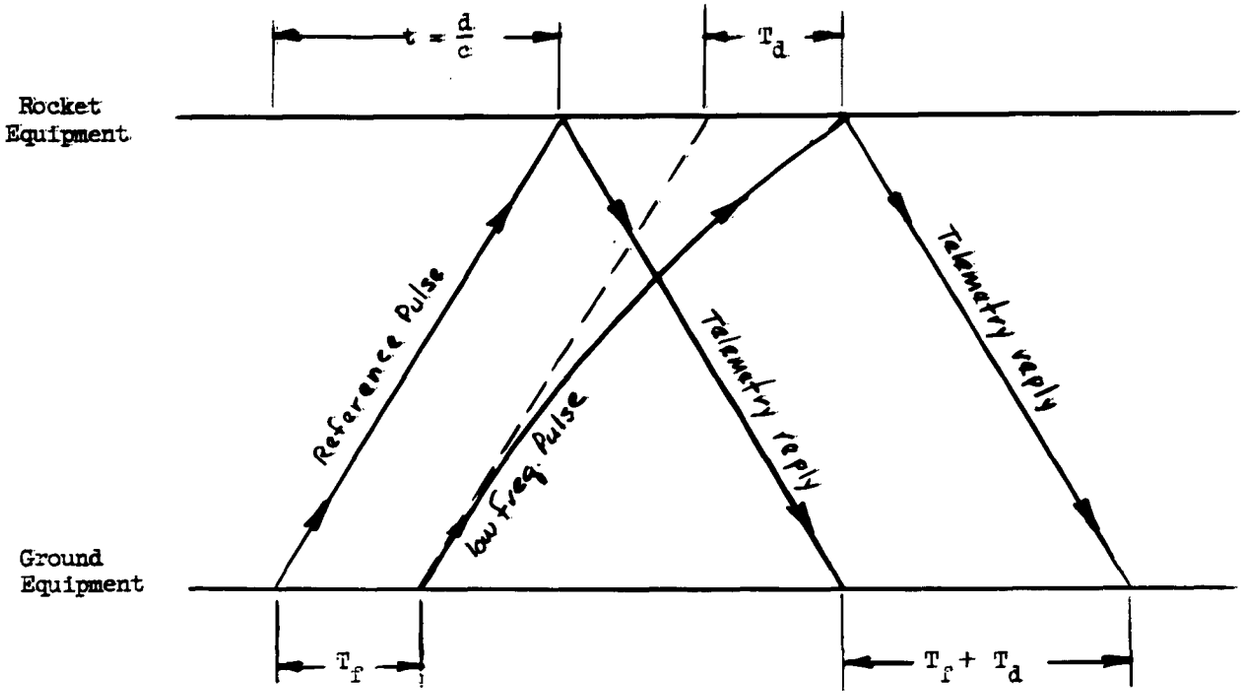

d = distance to rocket

c = velocity of light

T_f = fixed delay

T_d = relative retardation delay time

Fig. 2 Transmission Timing Sequence

III. THE REFERENCE LINK

We have already placed the requirement on the reference frequency that it must experience "negligible" change in group velocity in passage through the ionosphere. If the term negligible is taken to mean a maximum allowable change of 1%, then from the form of equation (2) it can readily be determined that the reference frequency must be in the order of 7 times greater than the plasma frequency of the medium. If the experiment is to be able to measure the electron density of the lower F layer of the ionosphere which exhibits a plasma frequency of about 10 mc, the reference frequency must be at least 70 mc or greater.

An s-band radar transponder was to be included in the rocket instrumentation to insure reliable tracking for good trajectory data. It was decided that it would be possible to utilize this transponder and the ground based radar transmitter and receiver to provide the reference link for the experiment. This required synchronization of the low frequency transmitter to the radar P.R.F. or an integral sub-multiple with a fixed time reference between transmission of the two pulses. Since the radar frequency is several orders of magnitude higher than the highest plasma frequency to be encountered in the ionosphere, its group velocity should exhibit freespace velocity for any practical measurement, and hence it should be an excellent reference. The combined functions of the UHF transmitter and receiver and the telemetry system of Fig. 1 are therefore actually performed by the radar system.

IV. THE PROBING FREQUENCY LINK

This part of the system consists of the ground based low frequency pulse transmitter, an airborne low frequency receiver and their associated antenna systems. The transmitter is to be considered in detail in a later section and thus will not be described here.

A. Airborne Low Frequency Receiver. The airborne receiver was in itself a challenging problem which was undertaken by Mr. Charles Alley, a faculty member of the Electrical Engineering Department of the University of Utah, during summer employment at the Upper Air Research Laboratory.

The Upper Air Research groupt agreed that the rocket-borne receiver should be designed to meet the following specifications:

Tuning range (with minor modification): 4 mc to 12 mc.
Bandwidth: 0.5 mc.
Sensitivity: 10 μ volts or better.
Frequency Stability: Assured by crystal controlled local oscillator.
Operating temperature range: 0 °C to 50 °C.
Antenna impedance: 50 ohms.
Outputs: Video and pulse at separate jacks.
Shocks and vibration. 100_g Shock, 20_g Vib. at 60 cps.

In addition to meeting the above specifications, the receiver was to be gated on for an adjustable 150 μs to 200 μs period following a 50 μs to 1 0 μs adjustable delay from a trigger pulse. Also, transistor circuits were to be used exclusively.

The requirement that the receiver be compact and rugged virtually eliminated the use of conventional tuning circuits which could ordinarily

be used to tune from 4 mcs to 12 mcs in a single band. Therefore, the decision was made to divide the 4 mcs to 12 mcs frequency range into three bands and utilize slug tuned coils to tune through each band. The procedure for changing bands would be to replace the fixed tuning capacitors in the r-f amplifier and first detector stages of a superheterodyne circuit.

The bandwidth requirement of the receiver discouraged the employment of an intermediate frequency (if) below 4 mcs. Also, an i-f above 12 mc was undesirable because the power gain of the available transistors decreased about 7 db for each octave frequency increase in this region. Therefore, the decision was made to operate the receiver as a tuned radio frequency (trf) receiver in the frequency band of 4 mc. to 6 mc. Then the receiver could be operated as a superheterodyne receiver in the upper two bands utilizing an intermediate frequency of 5.0 mc.

THE R-F TUNER

The circuit diagram of the r-f amplifier is shown in Fig. 3. The

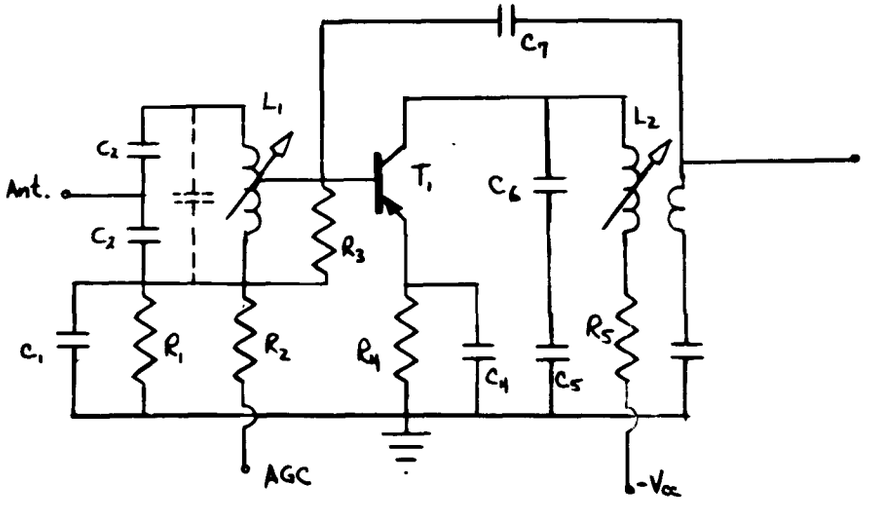

FIGURE 3. THE RF AMPLIFIER

capacitors C_2 and C_3 and the coil L_1 form the tuning and impedance matching network between the antenna input and the base of the transistor. The capacitor indicated by the dashed lines is added when reception in either of the lower two bands is desired. The resistors R_1, R_2 and R_4 comprise a stabilized bias circuit for the transistor. The values of these resistors are determined by the temperature stability requirements of the circuit. The automatic gain control (AGC) system reduces the forward bias on the transistor as the signal level increases. This reduced bias decreases the current gain and increases the input impedance of the transistor. Both of these effects decrease the power gain. The AGC system will be discussed later.

The 2N1742 was chosen as the transistor T_1. This choice was made because the input impedance of the 2N1742 is essentially independent of frequency over the 4 mcs. to 12 mcs. range. However, as previously mentioned, the input impedance is a function of the base bias. Therefore, the resistor R_3 was used to stabilize the load on the tuned circuit and hence, stabilize the bandwidth of the amplifier.

The capacitor C_7 provides neutralization for the transistor. The value of C_7 was determined by reference to the transistor manufacturers test circuit data.

The resistor R_5 is a decoupling resistor for the collector supply voltage V_{cc}. Capacitors C_1, C_4 and C_5 are bypass capacitors.

THE FREQUENCY CONVERTER

The circuit diagram of the frequency converter is shown in Fig. 3A. The biasing and decoupling circuits of the oscillator and first detector

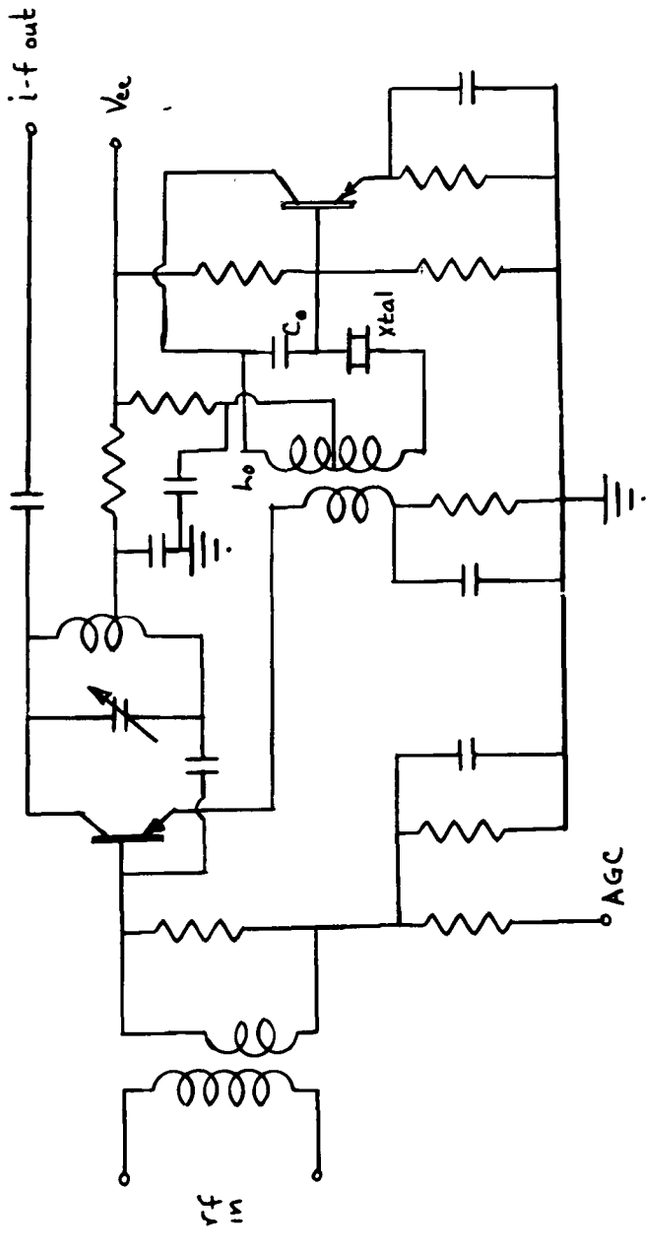

FIGURE 3A. THE FREQUENCY CONVERTER

are similar to these in the r-f amplifier circuit. The oscillator signal is inductively coupled into the emitter circuit of the first detector. The non-linearity of the input characteristics of the transistor is utilized to produce the sum and difference frequencies. The 2N1742 transistor is used in the first detector circuit.

The oscillator circuit is a Hartley circuit with the crystal operating in its series mode. Therefore, the frequency of oscillation will be very near the series resonant frequency of the crystal. The oscillation frequency will be precisely at this crystal frequency only when the inductance L_o and capacitance C_o also resonate at the crystal frequency. The oscillator frequency can be changed over fairly wide limits, however, without changing either L_o or C_o, because oscillation will occur when the crystal presents either a net capacitive or inductive reactance, providing this net reactance is appreciably smaller than the reactance of C_o. The crystal can provide this relatively small reactance only when the frequency of oscillation is very near the crystal resonant frequency. When the crystal is removed from the circuit, oscillations cease. However, the circuit will oscillate as a conventional LC Hartley circuit if the crystal is replaced either by a capacitance or a short circuit. When a capacitance is used to replace the crystal, the oscillator frequency will be controlled by the value of this capacitance. As the capacitance approaches the value of C_o, oscillation will cease. A 2N384 transistor was used in the oscillator.

THE I-F AMPLIFIER.

Preliminary calculations indicated that adequate receiver sensitivity would be achieved if two stages of i-f amplification were employed. Therefore,

are similar to these in the r-f amplifier circuit. The oscillator signal is inductively coupled into the emitter circuit of the first detector. The non-linearity of the input characteristics of the transistor is utilized to produce the sum and difference frequencies. The 2N1742 transistor is used in the first detector circuit.

The oscillator circuit is a Hartley circuit with the crystal operating in its series mode. Therefore, the frequency of oscillation will be very near the series resonant frequency of the crystal. The oscillation frequency will be precisely at this crystal frequency only when the inductance L_o and capacitance C_o also resonate at the crystal frequency. The oscillator frequency can be changed over fairly wide limits, however, without changing either L_o or C_o, because oscillation will occur when the crystal presents either a net capacitive or inductive reactance, providing this net reactance is appreciably smaller than the reactance of C_o. The crystal can provide this relatively small reactance only when the frequency of oscillation is very near the crystal resonant frequency. When the crystal is removed from the circuit, oscillations cease. However, the circuit will oscillate as a conventional LC Hartley circuit if the crystal is replaced either by a capacitance or a short circuit. When a capacitance is used to replace the crystal, the oscillator frequency will be controlled by the value of this capacitance. As the capacitance approaches the value of C_o, oscillation will cease. A 2N384 transistor was used in the oscillator.

THE I-F AMPLIFIER.

Preliminary calculations indicated that adequate receiver sensitivity would be achieved if two stages of i-f amplification were employed. Therefore,

two stages were designed using the 2N384 transistor. Since the two stages are identical, only one stage is shown in the circuit diagram of Fig. 3B. The second detector is also shown in this figure. Double tuned coupling circuits are used in the i-f amplifier. The value of the coupling capacitor C_c was chosen to provide a coefficient of coupling equal to 1.4 times the critical or transitional value. Then the selectivity pattern of the complete tuner is approximately that of two maximally flat triplets.

The transistor bias and tuned circuit loading in the i-f amplifiers are similar to their counterparts in the r-f amplifier. One additional feature has been added in the i-f amplifier, however. The resistors R_1 and R_2 in Fig. 3B provide a small bleeder current through the emitter circuit bias resistors. This current increases the effectiveness of the AGC system in reducing gain at high signal levels. Therefore the signal

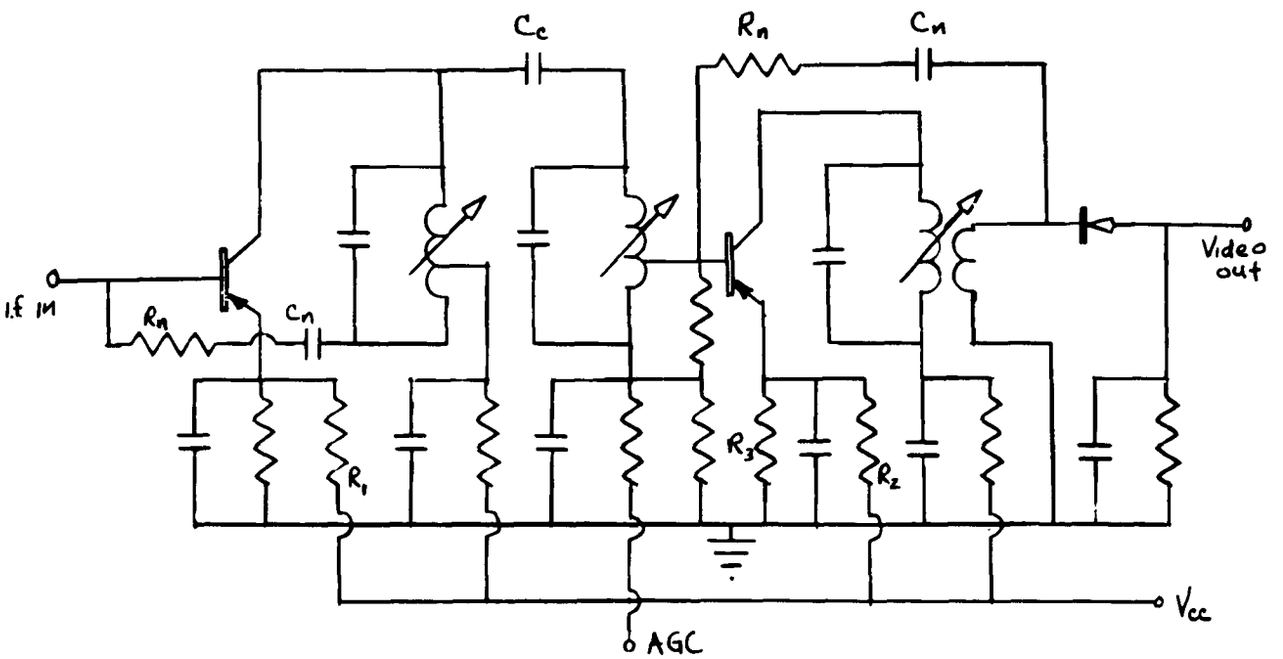

FIGURE 3B. THE i-f AMPLIFIER AND SECOND DETECTOR

level at which the receiver will saturate is increased because of this bleeder circuit.

THE VIDEO AMPLIFIER AND BLOCKING OSCILLATOR.

The criteria for selecting transistors for the video amplifier and blocking oscillator circuits were fast rise time, low saturation current I_{cbo} and moderate cost. In addition to providing adequate video gain, these circuits must provide the gating feature prescribed in the specifications. The circuit of Fig. 3C was devised to perform these functions. The component values are given in this figure to facilitate the understanding of the circuit operation. In the first video amplifier the 2.2 kΩ resistor in series with the base of Q_1 increases the charging time of the 0.1 μf coupling capacitor, thus reducing the reverse bias which results from the charging of this capacitor through the transistor

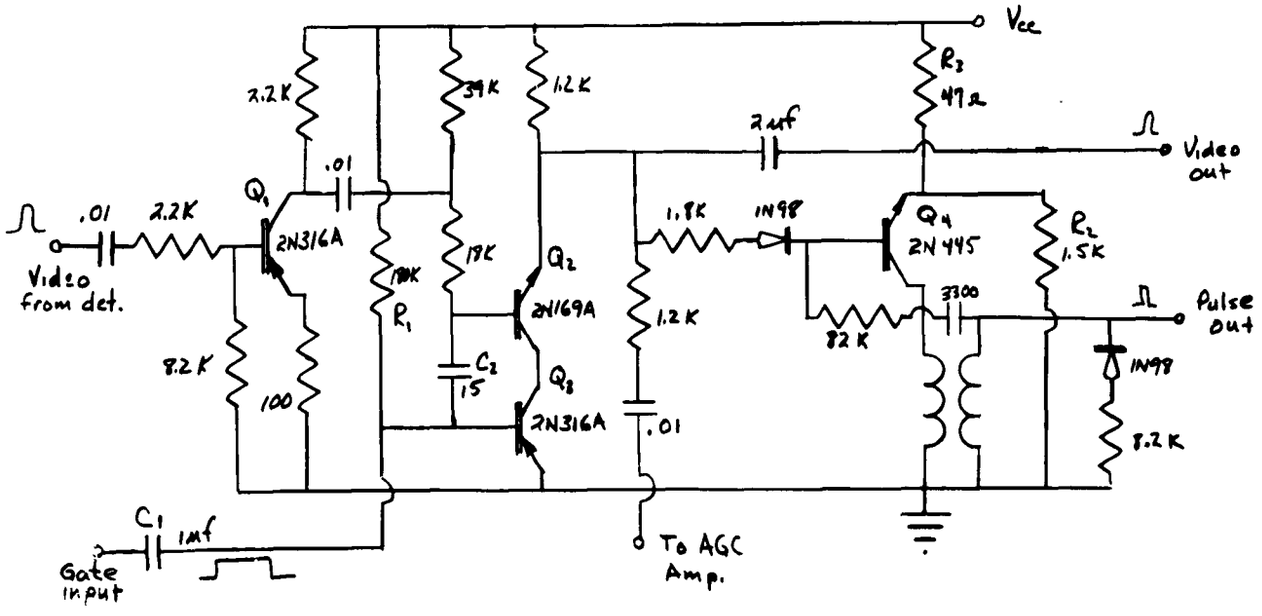

FIGURE 3C. VIDEO AMPLIFIER AND BLOCKING OSCILLATOR CIRCUITS

during the video pulse. A slight reverse base bias is beneficial because it eliminates the background noise or grass and thus improves the signal to noise ratio. This 2.2 k Ω resistor in series with the base also acts in conjunction with the input capacitance of the video amplifier to improve the filtering of the i-f from the video signal. The 100 Ω resistor in the emitter circuit of transistor Q_1 improves the thermal stability of this transistor.

The second video amplifier Q_2 operates as an emitter follower. The collector voltage of this transistor is supplied through the gating transistor Q_3 only during the gating pulse. Therefore, this second video amplifier Q_2 cannot amplify except during the time the gate pulse is applied to the gating transistor. However, the gating transistor is maintained in cut-off condition between gating pulses by the charge which accumulates on the capacitor C_1 during the gating pulse. Therefore, in case the gating pulse should fail, the gating transistor Q_3 would soon be forward biased to saturation by the current through R_1 and the receiver would operate continuously.

When collector voltage is not applied to the second video amplifier Q_2 the base signal is coupled through the forward biased base-emitter junction into the emitter circuit. In order to minimize this signal feed through during the off period of the gate, the 18 kΩ resistor was added in series with the base. This increased driving source resistance has little effect on the output signal while the amplifier is gated on because the amplifier then has a very high input impedance.

Without the capacitor C_2 the leading edge of the gating pulse fed

through the collector junction capacitance of transistor Q_2 and caused a very narrow spike to appear in the output. Therefore, the small capacitance of C_2 was added to the circuit to couple a spike of similar characteristics but opposite polarity into the base of transistor Q_2. Thus the gating spike was essentially eliminated by the addition of C_2.

The gated video from the emitter follower is coupled through resistors to the AGC amplifier and the blocking oscillator circuit in addition to being capacitively coupled to the video output jack. The diode in the base circuit of the blocking oscillator Q_4 provides uni-directional coupling to the blocking oscillator. Without this diode the base voltage of the blocking oscillator would be coupled into both the AGC amplifier and the video output. The resistor R_f in series with the blocking oscillator feedback capacitor prevents overshoot of the base pulse. Base pulse overshoot would be coupled back into the video and AGC circuits.

The bleeder current through resistor R_2 (1.5kΩ) flows through resistor R_3 and applies a small reverse bias to the emitter of the blocking oscillator transistor Q_4. The value of this reverse bias determines the triggering level of the blocking oscillator. The series diode and resistor combination across the output of the blocking oscillator transformer damps out the oscillations and overshoot of the pulse transformer.

THE AGC SYSTEM

The AGC system must be sensitive to the amplitude of the video pulse but insensitive to the background interference in the receiver. Therefore, the gated video pulse is used to activate the AGC system. Also, as shown in the circuit diagram of Fig. 3D, the AGC amplifier is capacitively coupled;

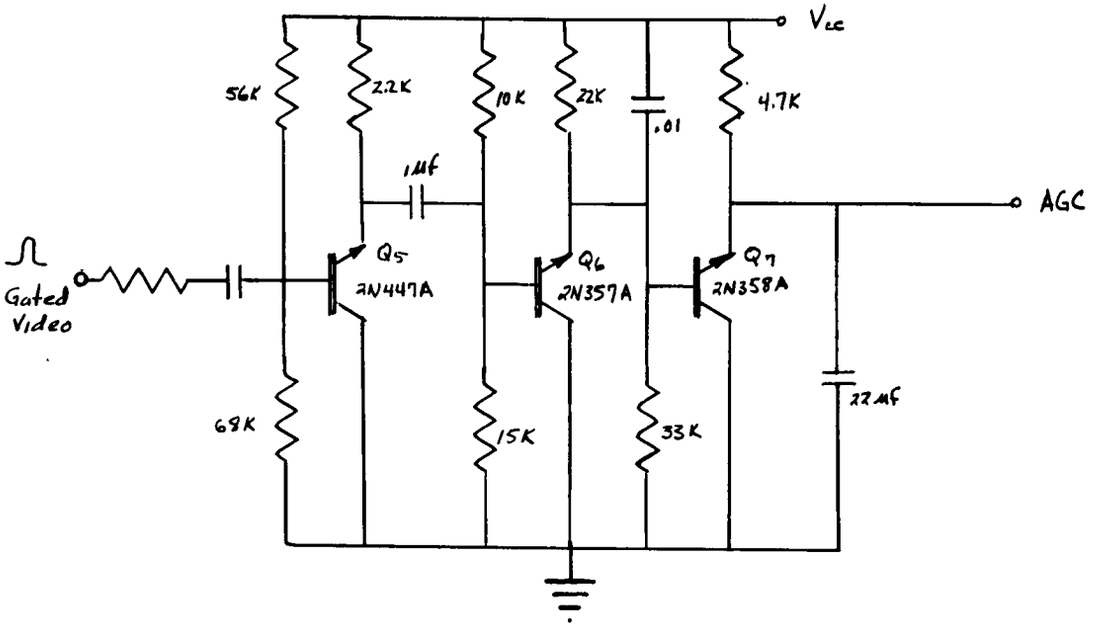

FIGURE 3D. THE AGC AMPLIFIER

hence cw signals cannot activate the AGC system. The AGC amplifier consists of three cascaded emitter followers which provide a very low output impedance and a high input impedance. The operating point of each of these amplifiers is in a slightly reverse base bias condition under quiescent conditions. Therefore, when no input signal is present, the r-f and i-f amplifiers obtain normal forward base bias through the AGC system and the 4.7k resistor R.

When a video pulse is applied to the AGC amplifier, each transistor is forward biased during the period of the pulse. During this time the 22 μf capacitor C discharges through the very low output resistance of transistor

Q_7. The discharge time constant of capacitor C through the output resistance of transistor C_7 must be of the same order of time as the duration of the video pulse. However, the capacitor C charges through the 4.7 kΩ resistor R during the time between video pulses. The charging time constant is the product of the capacitance of C and the parallel combination of resistance R and the resistance between the AGC line and ground. This time constant must be long in comparison with the video pulse repitition frequency so the AGC voltage will not change appreciably between video pulses.

The capacitor in the emitter circuit of transistor Q_6 broadens the video pulse and thus reduces the peak currents through transistor Q_7. The small input current to transistor Q_5 cause no significant loading on the video amplifier during the video pulse. The AGC voltage reduction from the quiescent condition is almost equal to the voltage amplitude of the video pulse applied to the AGC amplifier.

THE DELAY AND GATING CIRCUITS.

The delay and gating circuits are conventional monostable multivibrator circuits as shown in Fig. 3E. The reference diode in the input of the delay circuit clips the input trigger level at 7.0 volts and thus protects the transistors from excessive voltages in addition to providing a relatively constant trigger amplitude. The sensistors in the emitter circuits of the multivibrators cause the delay and gate lengths to be essentially independent of temperature. The output impedance of the gating multivibrator must be fairly low in order to charge the coupling capacitor C_1 during the gate interval. As explained in the video amplifier section this charging of

C_1 is necessary in order to keep the video amplifier disabled between gating pulses.

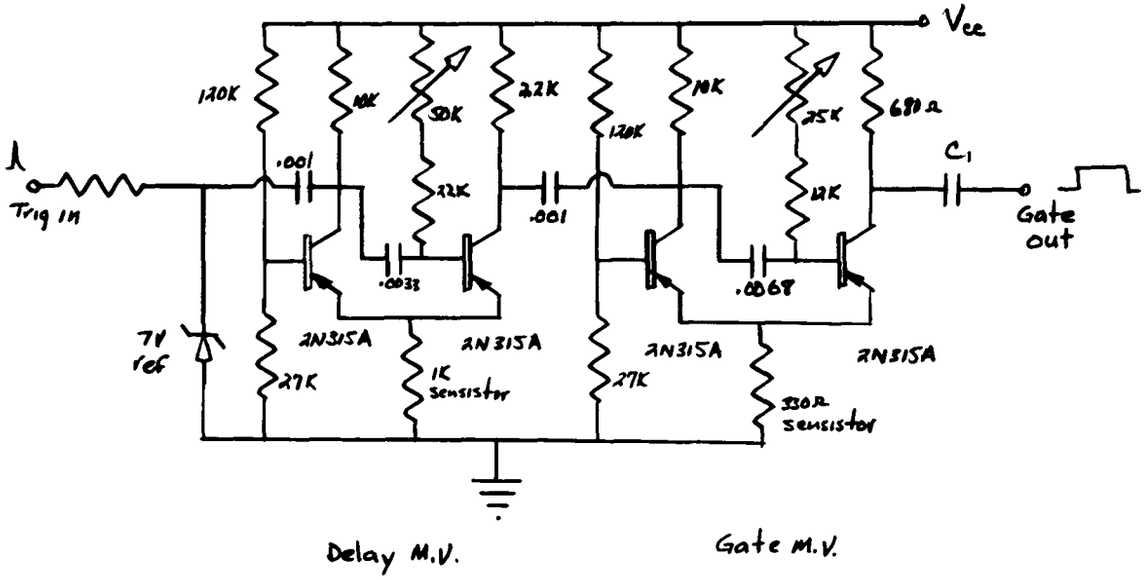

FIGURE 3E. THE DELAY AND GATING CIRCUITS

TEST RESULTS

The receiver was tested in a varying temperature environment. The receiver sensitivity, bandwidth, output pulse amplitude, delay time, gate width and supply current drain were measured as a function of temperature from -10° centigrade to 60° centigrade. The output pulse amplitude remained constant at 62 volts. The current drain also remained constant at 35 ma. Therefore, the total power drawn from the power supply is nominally 420 milliwatts. The variations of sensitivity and bandwidth as functions of temperature are shown in Fig. 3F. The sensitivity met the specifications

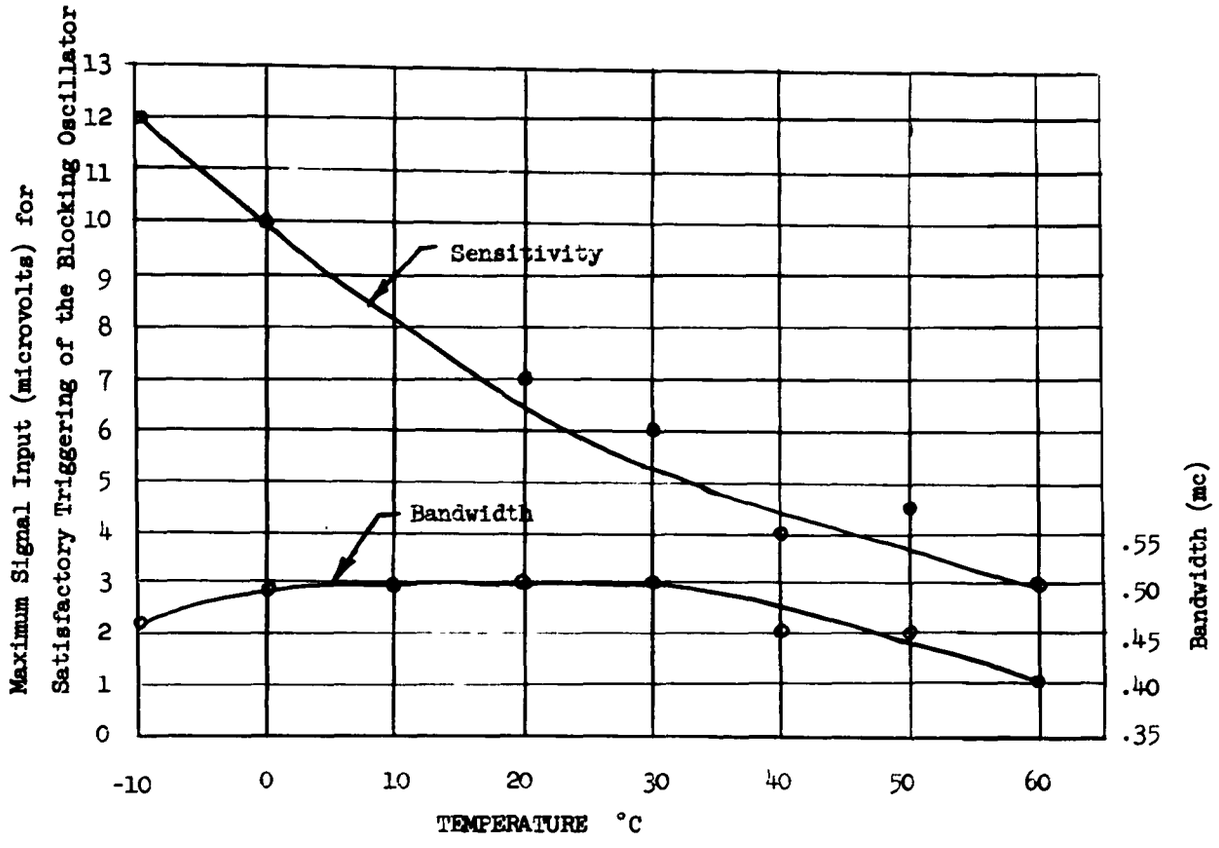

FIGURE 3F.

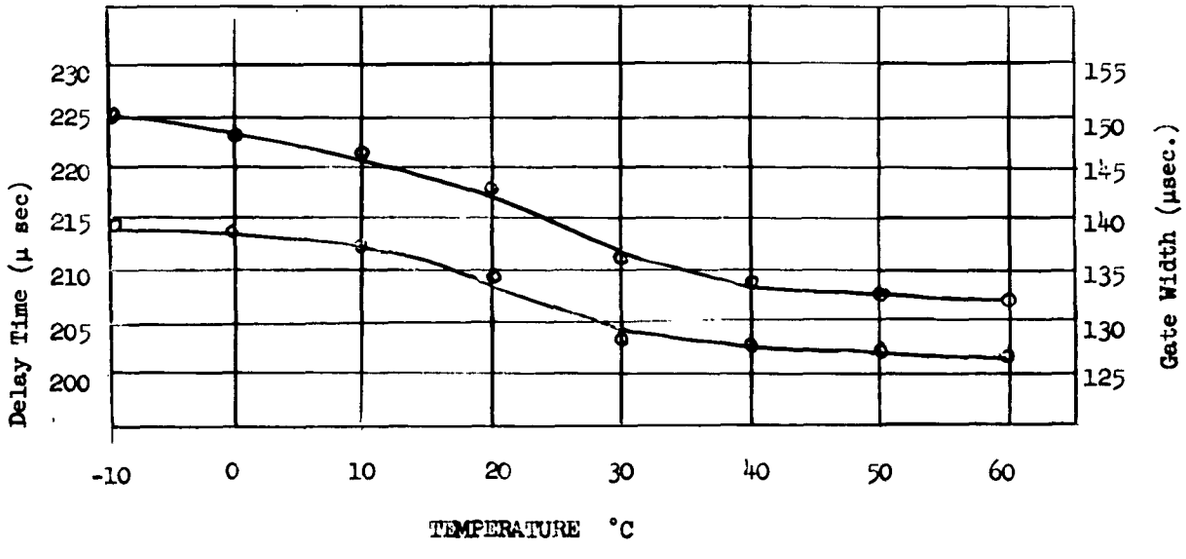

FIGURE 3G. RECEIVER CHARACTERISTICS VS. TEMPERATURE

over the prescribed temperature range. However, the bandwidth decreased from approximately 0.5 mc at moderate temperatures to 0.45 mc at the upper prescribed limit of 50° C. Although the 0.45 mc bandwidth is satisfactory, the bandwidth of the production models will be increased sufficiently to provide 0.5 mc minimum bandwidth.

The delay time and gate width are plotted as functions of temperature in Fig. 3G. The delay time varied approximately 7 percent and the gate width varied about 8 1/2 percent over the prescribed temperature range. The decrease in delay time and gate width with increasing temperature indicates that the multivibrators are over compensated. The variations of delay time and gate width with temperature could be reduced to less than 5 per cent if the proper amount of fixed resistance were combined with the sensistors to reduce the amount of compensation. The complete schematic diagram of the receiver is presented in Fig 3H. Also, photographs which show the receiver construction details are provided in Fig. 4.

B. Low Frequency Receiving Antenna. The airborne low frequency receiving must meet some very exacting mechanical as well as electrical requirements. If there is any protrusion on the outside of the rocket skin, it must be of such size and design that the aerodynamic properties of the missile are not appreciably altered. Also, any protrusion into the air stream may experience severe frictional heating as the missile passes through the dense portion of the atmosphere. Indications from previous experiments are that such protrusions may experience surface temperatures as high as 1000°F. An antenna structure must also be mechanically strong enough to survive the heavy vibrational and acceleration environment during the

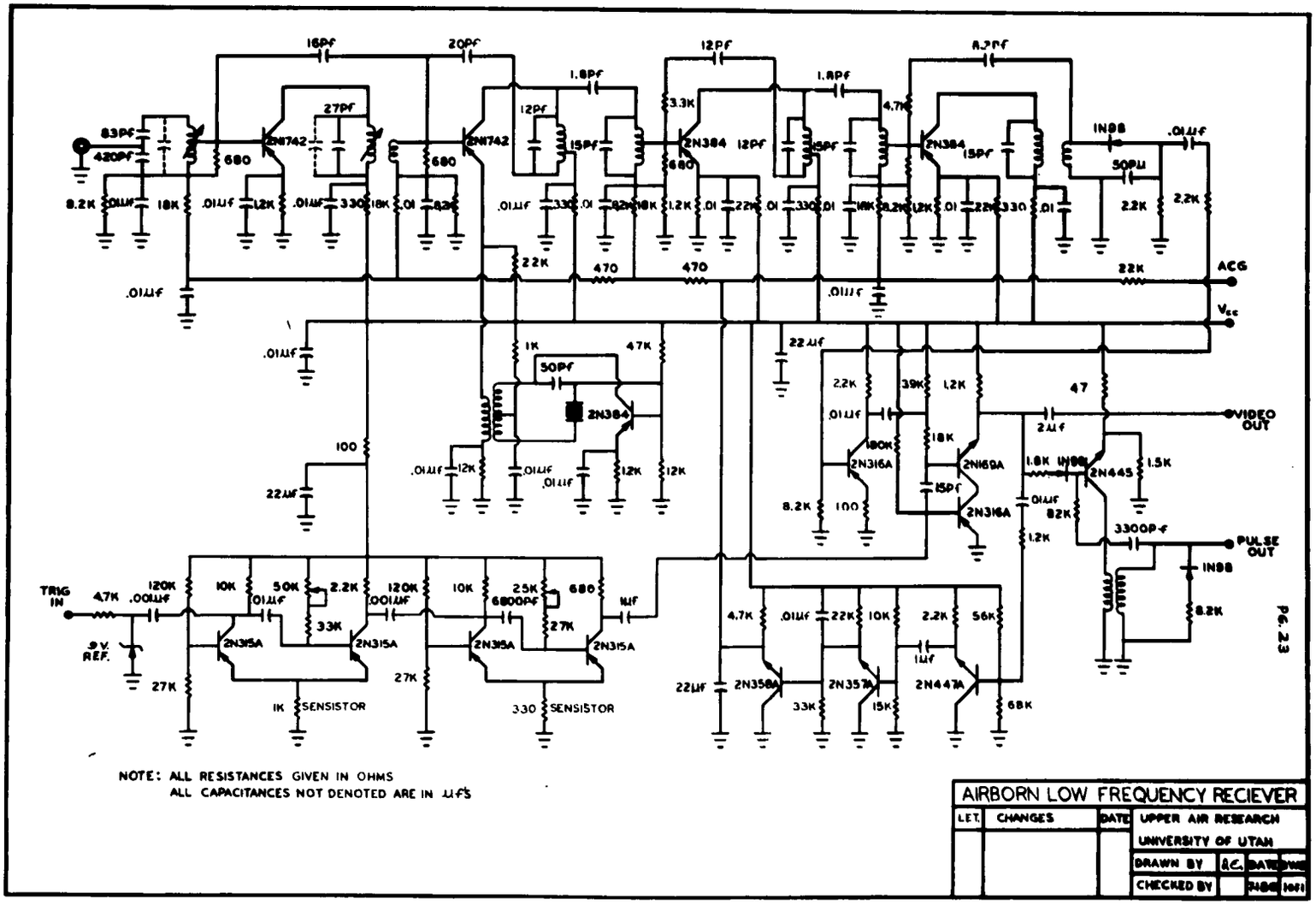

FIGURE 3H. SCHEMATIC SIGNAL OF LOW FREQUENCY RECEIVER

A.

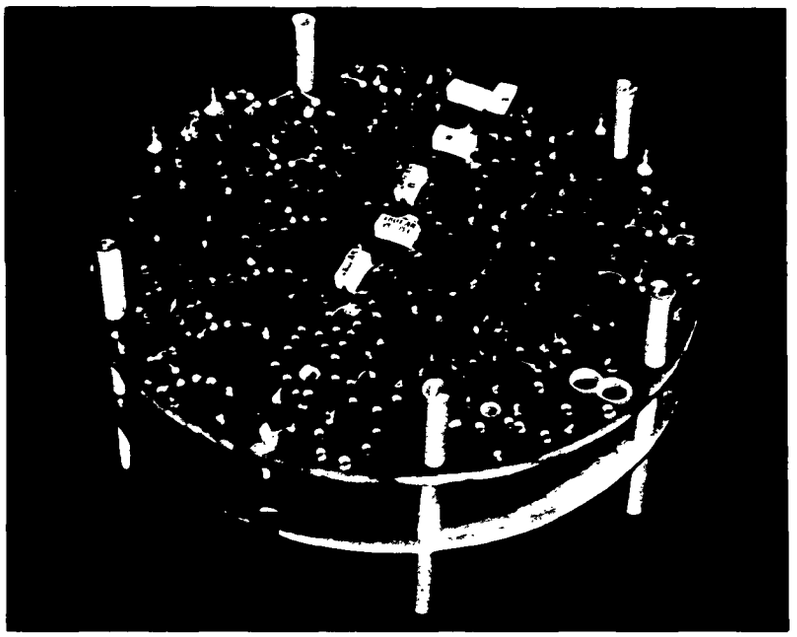

B.

FIGURE 4, CONSTRUCTION DETAILS OF AIRBORNE LOW FREQUENCY RECEIVER

powered portion of the rocket flight. It is desirable that the antenna mechanism be as simple as possible to insure the greatest reliability of operation.

Eletrically, the low frequency antenna must be some appreciable fraction of a wavelength in order to achieve a high degree of efficiency. For the range of specified operating frequencies, the electrical wavelengths vary from 25 meters to 75 meters. Since the missile to be used for conducting the experiment has an overall length of approximately 10 meters, the design of an efficient antenna system is indeed a difficult problem. Various low frequency antenna systems have been used in conducting other previous experiments and evaluation studies of their performance characteristics have been made.[4,5] Of these, the system which was chosen for this experiment was a dipole antenna consisting of two 8 foot fiberglass covered whips to be mounted on diametrically opposite sides of the missile. An erection mechanism has been developed which allows the antennas to remain flat against the rocket body during the initial part of the flight. In this position a streamlined profile is presented to the air stream by an aluminum casting into which the antennas are mounted. The antenna mounting and erection mechanism is shown in Figures 5 and 6 and the complete assembly with the fiber-flass antennas in flight position is shown in Fig. 7. At a predetermined time, the mechanism is tripped and the antennas are erected by spring tension.

---

[4] G.F. Miner, "Characteristics of Low Frequency Antennas for Rocket Applications", M.S. Thesis, Electrical Engineering, University of Utah; 1960.

[5] K.D. Baker, "High-Altitude Rocket Loop Antennas", M.S. Thesis, Electrical Engineering, University of Utah; 1957.

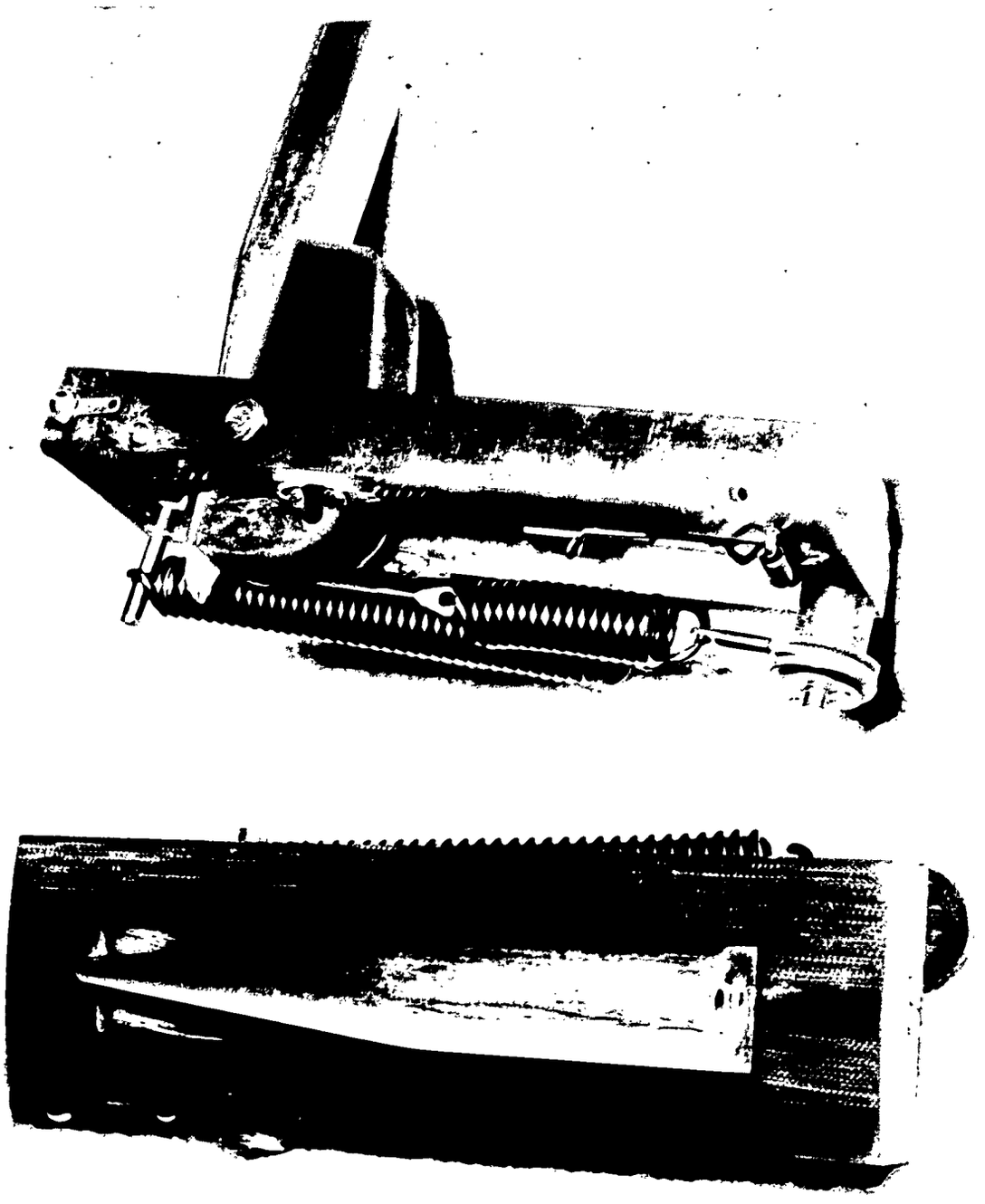

FIGURE 5. ANTENNA MOUNTING AND ERECTION MECHANISM

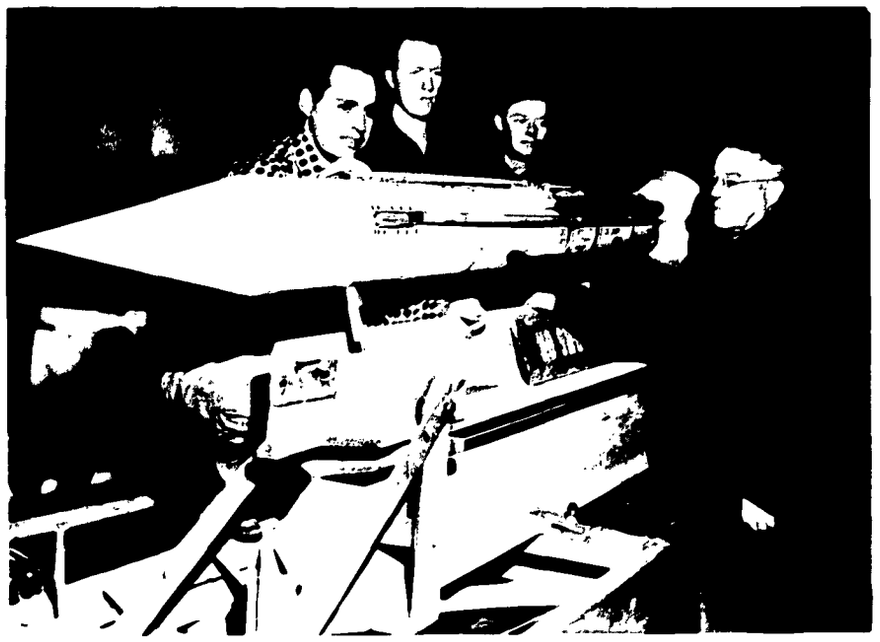

FIGURE 6. ANTENNAS MOUNTED ON ROCKET BODY

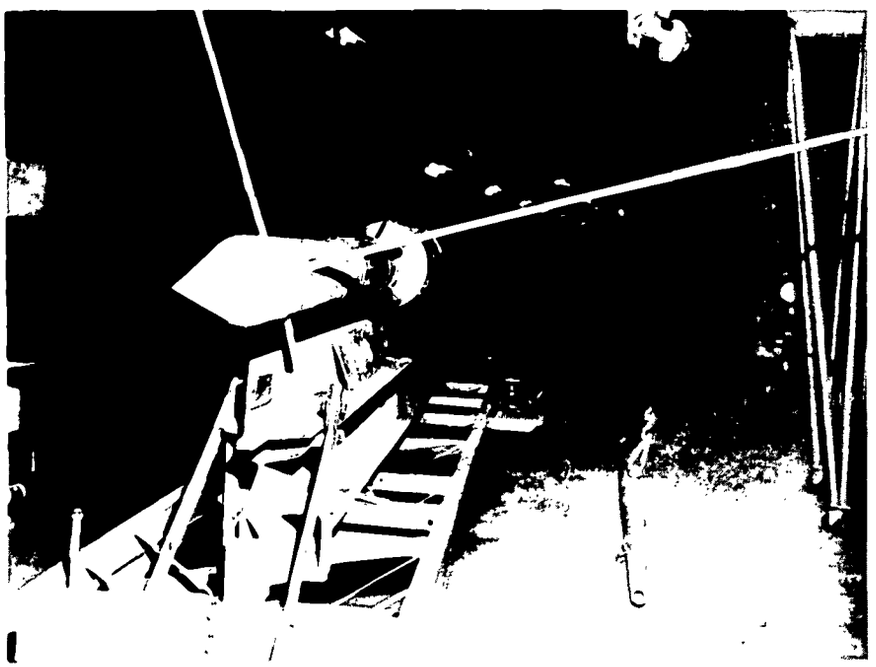

FIGURE 7. ANTENNAS EXTENDED IN FINAL POSITION

The spring must only be capable of overcoming the friction in the system and a slight amount of air drag. The rocket will be above the major portion of the atmosphere and essentially in a free fall condition when the antennas are released.

The antenna elements are so constructed that the lower section consists of a distributively wound coil which gives approximately the right inductive component to resonate the electrically short antenna slightly above the desired operating frequency. A final tuning of the antenna can then be accomplished by inserting ferrite material into the base of the antenna thus increasing the inductive component of the distributed coil to resonate the antenna at the desired frequency.[6] This tuning operation is conducted by placing 1/2 of the dipole on a mockup of the actual rocket body with an infinite ground plane passing through the center neutral plane. The terminal impedance is measured with an impedance bridge located in an excavation directly beneath the antenna and the ground plane.[7]

This type of antenna should prove very satisfactory in all respects. The impedance characteristics indicate the bandwidth to be sufficient and the efficiency is superior to that of a straight dipole antenna of the same length which is tuned by a lumped inductor. The fiberglass coating on the surface of the antenna provides adequate protection from the frictional heating to be expected as the missile passes through the dense portion of the atmosphere.

---

[6] Miner, op. cit., p. 24

[7] Ibid., p. 30

V. THE RECORDING STATION

Requirements for reduction of the data from the primary quantity of pulse delay time to electron density of the medium make it desirable to be able to measure the propagation delay of the low frequency pulse to the order of .1 μsec accuracy. This requirement virtually eliminates all common methods of recording the data other than direct photographing of an oscilloscope display. A block diagram of the ground recording equipment is shown in Fig. 8.

Coincident with the upward transmission of the low frequency pulse, a 2000 μsec gate is initiated which places the sweep trigger circuit in a state such that it will accept the first incoming pulse which is of the proper amplitude. The gate length of 2000 μsec was selected as the maximum estimated time which should be required for propagation of the low frequency pulse from the ground to the rocket and the return of the high frequency reply when the rocket is at peak altitude. If the system pulse repitition frequency is about 200, the gate will eliminate the possibility of noise triggering over somewhat greater than half the total period between pulses, thus giving an overall noise reduction factor of about 2. This figure could be greatly increased if it were possible to employ some type of coding on the reference pulse. With the use of the radar system as the reference link, this cannot be accomplished and the factor of two is about the best that can be achieved without sacrificing data points by using a lower P.R.F.

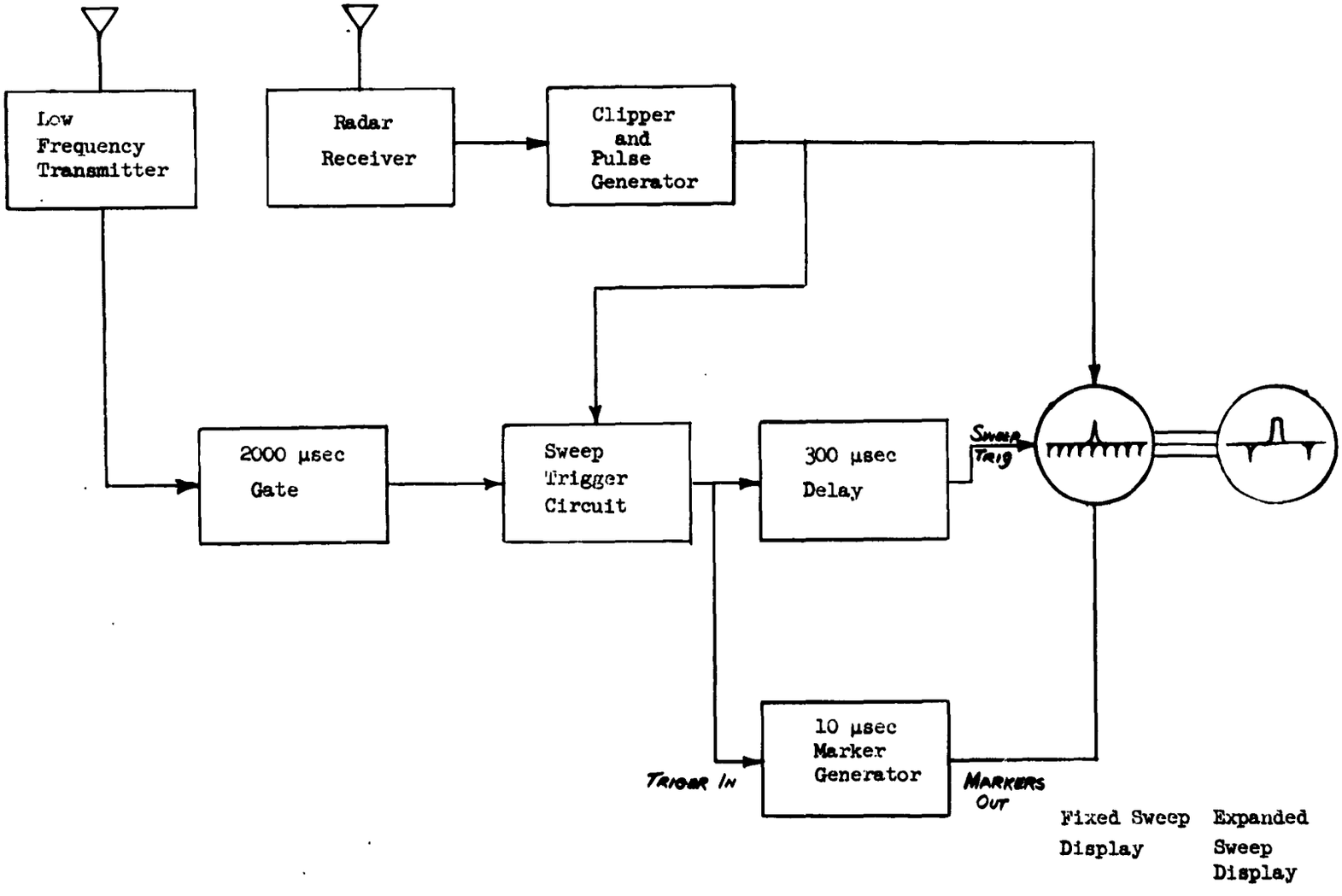

Figure 8. GROUND STATION

The clipper and pulse generator consists primarily of a blocking oscillator which incorporates a clipping circuit so that only pulses of a given amplitude will be accepted from the radar receiver.

The output of this unit is sent to the vertical plates of the oscilloscopes and also to the sweep trigger circuit. This circuit produces a trigger upon receipt of the first pulse after the 2000 μsec gate is initiated. For good signal strength at the radar receiver, this will be the reference pulse. The sweep trigger circuit is designed with a recovery time of 500 μsec to prevent the data pulse from also triggering the oscilloscope sweep. The schematic of the pulse generator, 200 μsec gate, and sweep trigger circuit is shown in Fig. 9. The output of the sweep trigger circuit must then be delayed 300 μsec before triggering the oscilloscopes. This delay corresponds to the initial fixed delay between the upward transmission of the high and low frequency pulses, which was represented graphically as T_f in Fig. 2. Ten μsec range markers are generated by a ringing type marker generator and mixed with the radar receiver video to be displayed vertically on the oscilloscopes. The marker generator is triggered by the output of the trigger circuit directly, thus eliminating any possibility of jitter due to the delay circuit. The 300 μsec delay circuit is shown in Fig. 10 and the marker generator in Fig. 11.

Recording the data consists of photographing each trace of an oscilloscope by means of a 35 mm moving strip camera. It is proposed to use two oscilloscopes in parallel. One uses a fixed sweep length corresponding to the largest pulse delay which is likely to be encountered during the flight, and the other is an expanded sweep type which displays only a

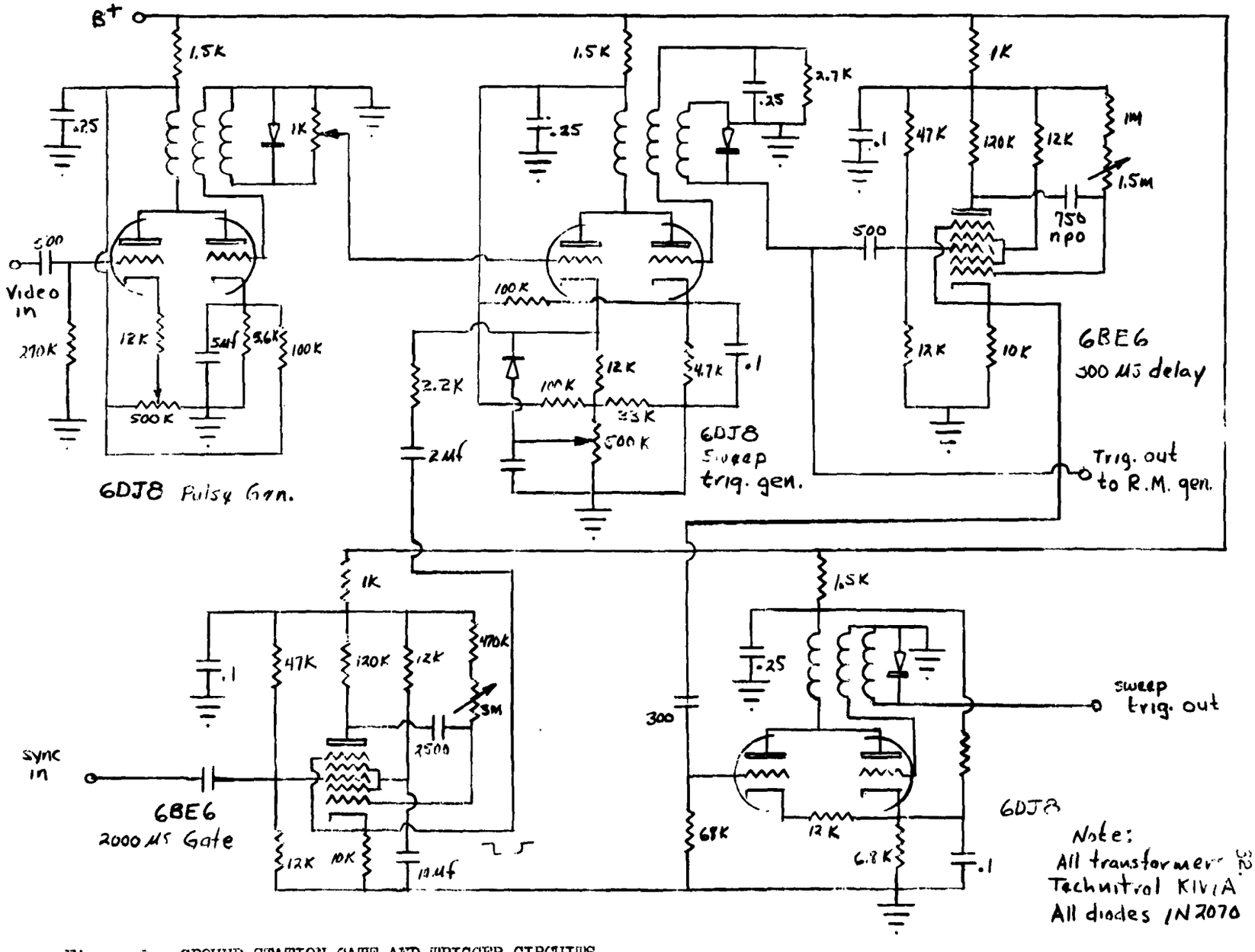

Figure 9. GROUND STATION GATE AND TRIGGER CIRCUITS

small region around the data pulse. With this oscilloscope, an operator must be present to continually advance the delay and "follow" the data pulse as the relative delay time is varied by the ionosphere. A high degree of accuracy can be obtained by comparing corresponding traces on the two oscilloscopes. The display with the long sweep length can be used to locate a range marker nearest the data pulse and this can then be used for a more accurate measurement of the pulse delay time from the expanded sweep trace.

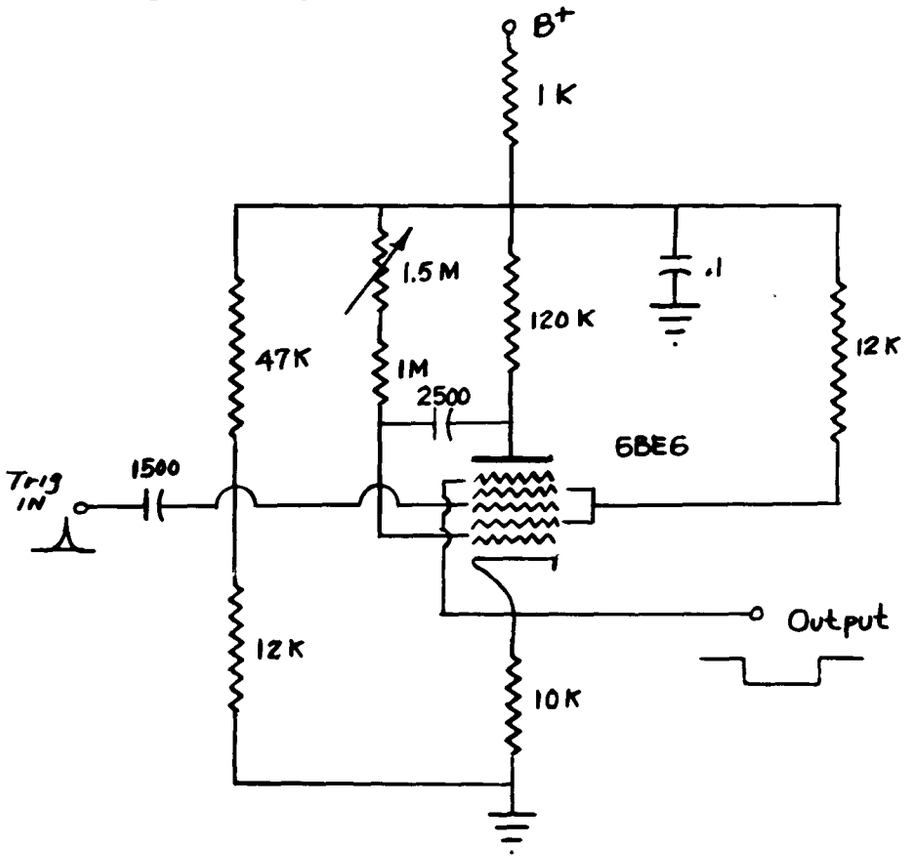

Figure 10. PHANTASTRON DELAY

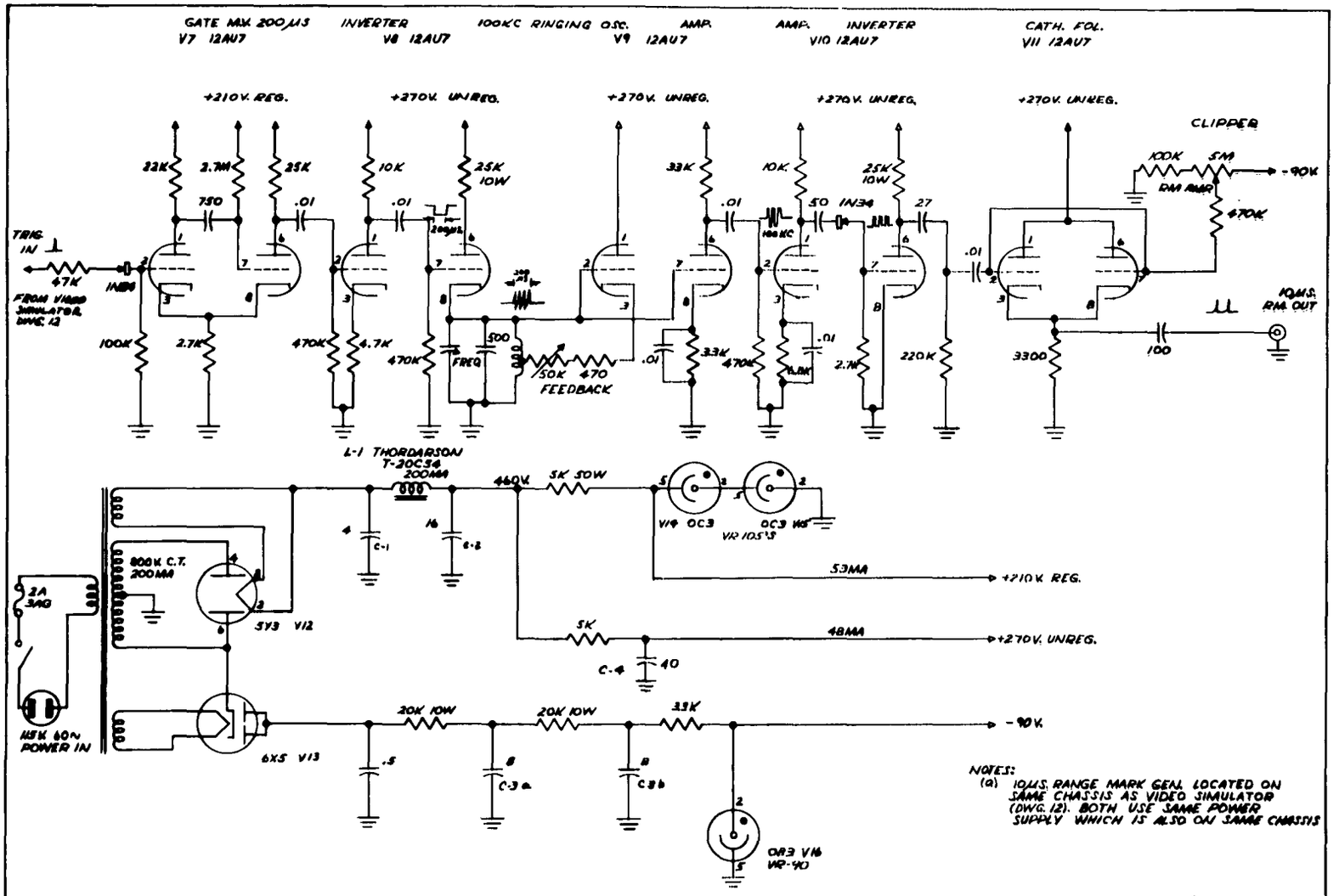

FIGURE 11. 10 μsec RANGE MARK GENERATOR

VI. THE LOW FREQUENCY TRANSMITTER

A block diagram of the low frequency transmitter is shown in Fig. 12. Its basic operation will now be briefly discussed and then each of the units will be examined in detail.

The input trigger, which is coincident with the transmission of the high frequency reference pulse, is clipped and the pulse repetition frequency counted down if desired in Unit A. This circuit can also be made to free run, for testing purposes, with an adjustable P.R.F. by the closing of a switch so that the transmitter will operate in the absence of an input trigger. The trigger then initiates a delay circuit (B) which provides an adjustable delay between the transmission of the reference pulse and the low frequency pulse. The delayed trigger is then distributed to a gated pulse generator (C) and to a staircase generator (D). The staircase generator includes a count— down circuit for allowing a desired number of pulses for each step position and an additional delay which positions the staircase such that the modulating pulse will occur on the flat portion of each step. A pulse is also produced at the beginning of each stepping sequence which triggers the coding gate circuit (E). This, in turn, biases the blocking oscillator off for a period of one step width. Coding of the output pulse train is thus accomplished by blanking the pulses from the bottom step in each stepping sequence. This coding makes it possible to readily determine the frequency of each pulse in the recorded data. The staircase waveform is used to frequency modulate an oscillator (F) producing the desired frequency stepping feature. The oscillator output passes through a low level cw amplifier before being pulse modulated and fed to the power amplifier.

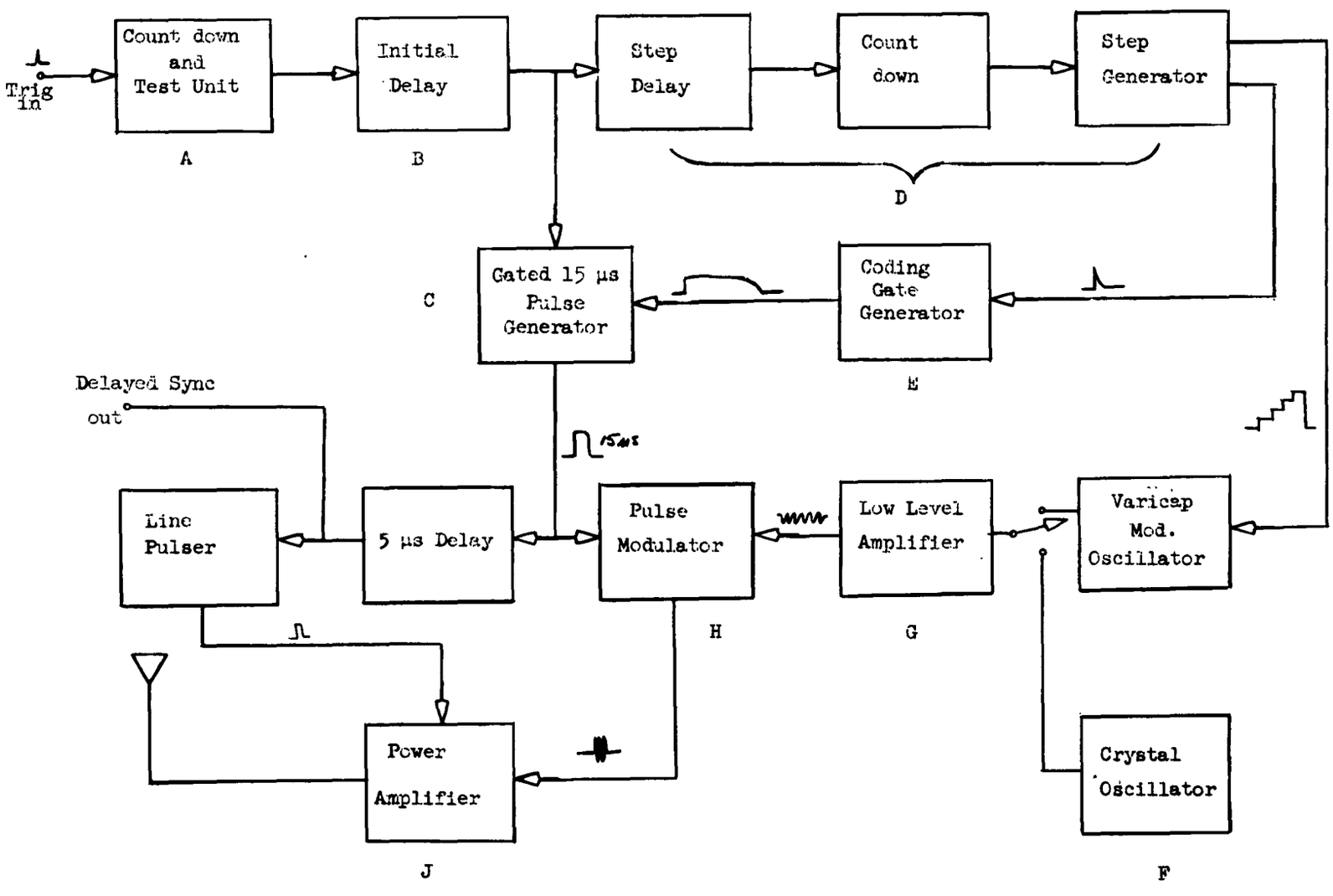

Figure 12. LOW FREQUENCY BLOCK DIAGRAM

A. Countdown and Test Unit. The circuit for this unit is shown in Fig. 13. It constitutes a common triggered blocking oscillator, which employes a dual triode to isolate the trigger input. The clipping feature is provided by varying the bias on the input tube, V_1. The blocking oscillator tube, V_2, is normally biased beyond cutoff and fires only on a trigger of the proper magnitude. A countdown feature is provided by the adjustable grid recovery circuit R_1, C_1. When switch S_1 is closed, the fixed bias is removed from V_2 and the circuit free runs with a repetition rate which is determined by $R_1 C_1$.

B. Initial Delay and Staircase Generator. The initial delay and the step delay are both provided by cathode coupled phantastron delay circuits, which are identical to that of Fig. 10. This circuit is widely used[8] and need not be further discussed here except to mention that care must be taken to insure that capacitor C_1 be temperature stable to eliminate drift and jitter. If this precaution is made, a jitter in the order of .1μs may be expected for a total delay time of several hundred μs.

The generation of the staircase waveform is accomplished by the circuit of Fig. 14. A blocking oscillator is used in conjunction with a bi-stable four layer transistor diode.* The transistor diode is the solid

---

[8] Millman and Taub, "Pulse and Digital Circuits", McGraw Hill Book Co., Inc., New York, New York, P. 225-7; 1956

*Advice produced by Shockley Transistor Corp., Palo Alto, Calif. Refer to Bulletic No. AD-2, February 1959.

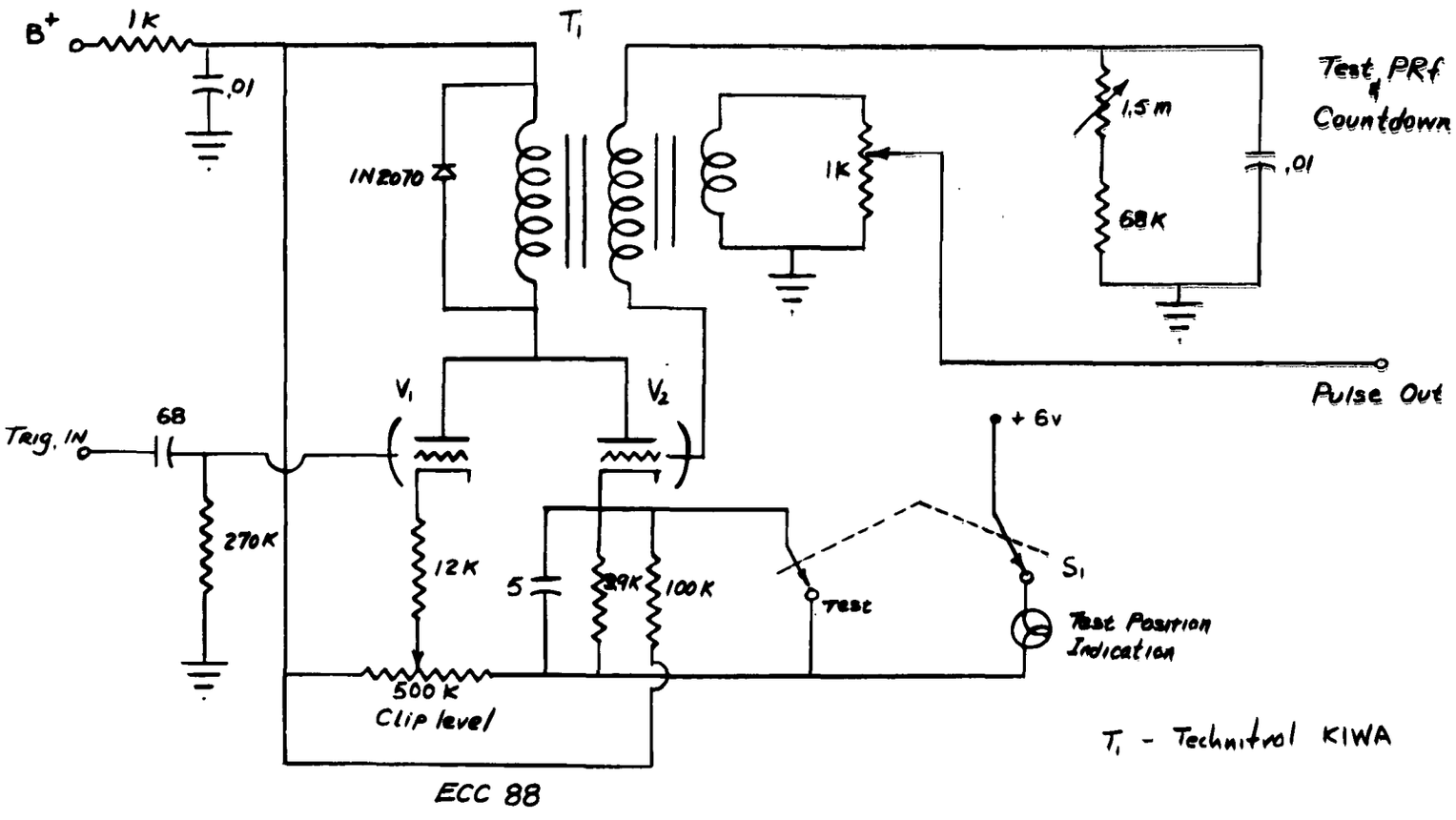

Figure 13. COUNTDOWN AND TEST UNIT

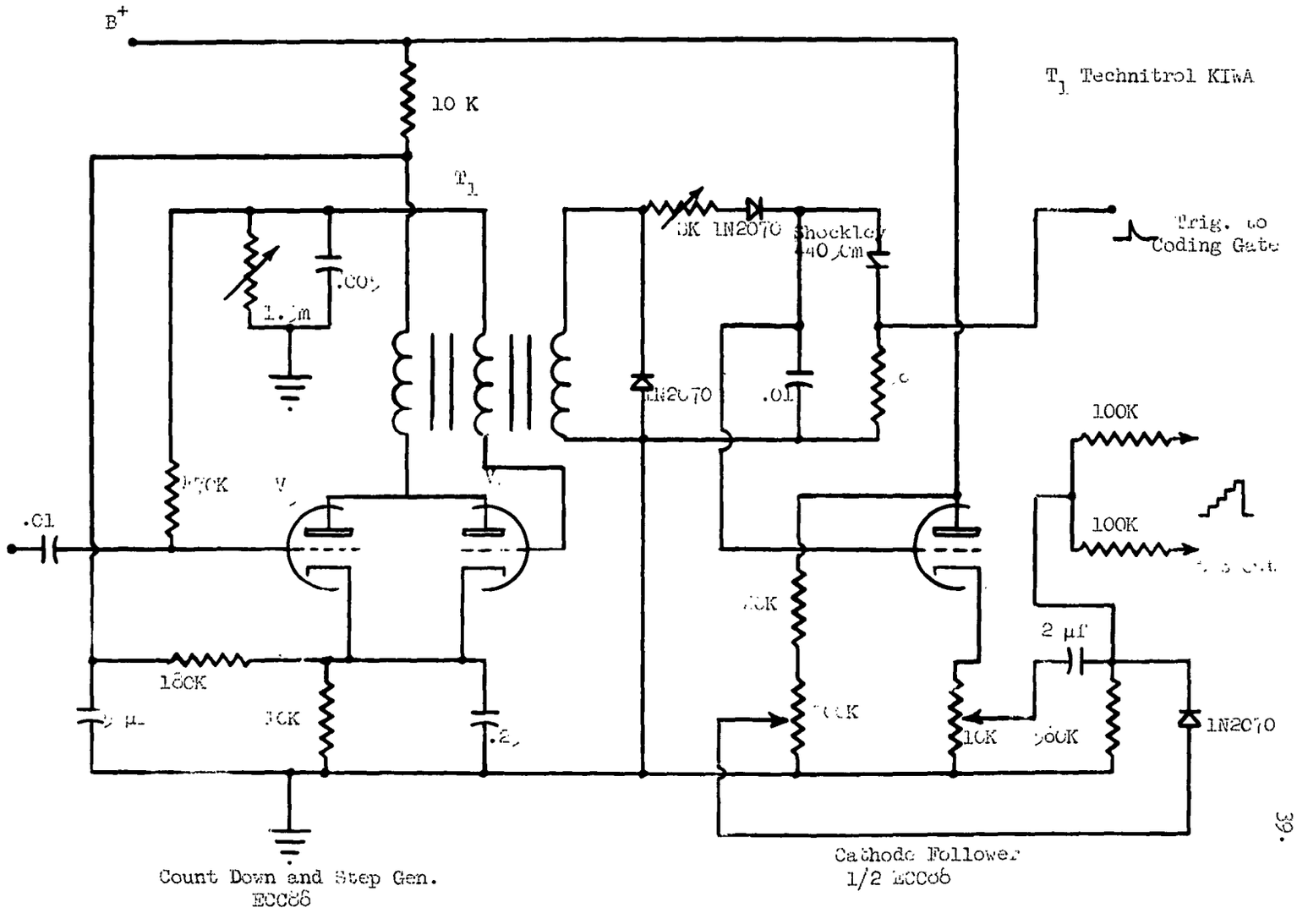

Fig. 14. Staircase Generator

state equivalent of a gas discharge tube; it maintains a very high impedance until a critical voltage is reached at which point it breaks down and becomes a very low impedance. It remains in this state until the current reduces to a minimum level where it again switches to the high impedance condition. The blocking oscillator pulses are integrated by C_1 until the breakdown level of the transistor diode is reached. The capacitor is then discharged through the diode and R_2 producing a pulse which is used to trigger the coding gate circuit. The number of pulses which must be integrated to reach the breakdown level, and hence the number of steps, is controlled by R_1 which limits the current flow into C_1 during each pulse. An adjustable grid recovery circuit is also incorporated in the blocking oscillator to allow each step width to be an integral number of pulse spaces. Ultimately, this allows an integral number of successive pulses at each frequency in the stepping sequence.

C. Coding and gate circuits. The function of this circuit is to code the output pulse train by blanking one or more pulses at the beginning of each stepping sequence, thus providing a reference for identifying the various frequencies when reducing the data. A diagram of this portion of the transmitter circuitry is shown in Fig. 15. The coding gate is produced by a phantastron circuit, V_7, which is identical to those which were used for delay functions, except the output is taken from the common grids 2 and 4 as a positive pulse is desired in this case.

The 15 μs pulse generator is a triggered blocking oscillator, which uses a dual triode to isolate the input trigger. The positive coding gate is applied to the cathode circuit of the trigger tube V_8, thereby biasing

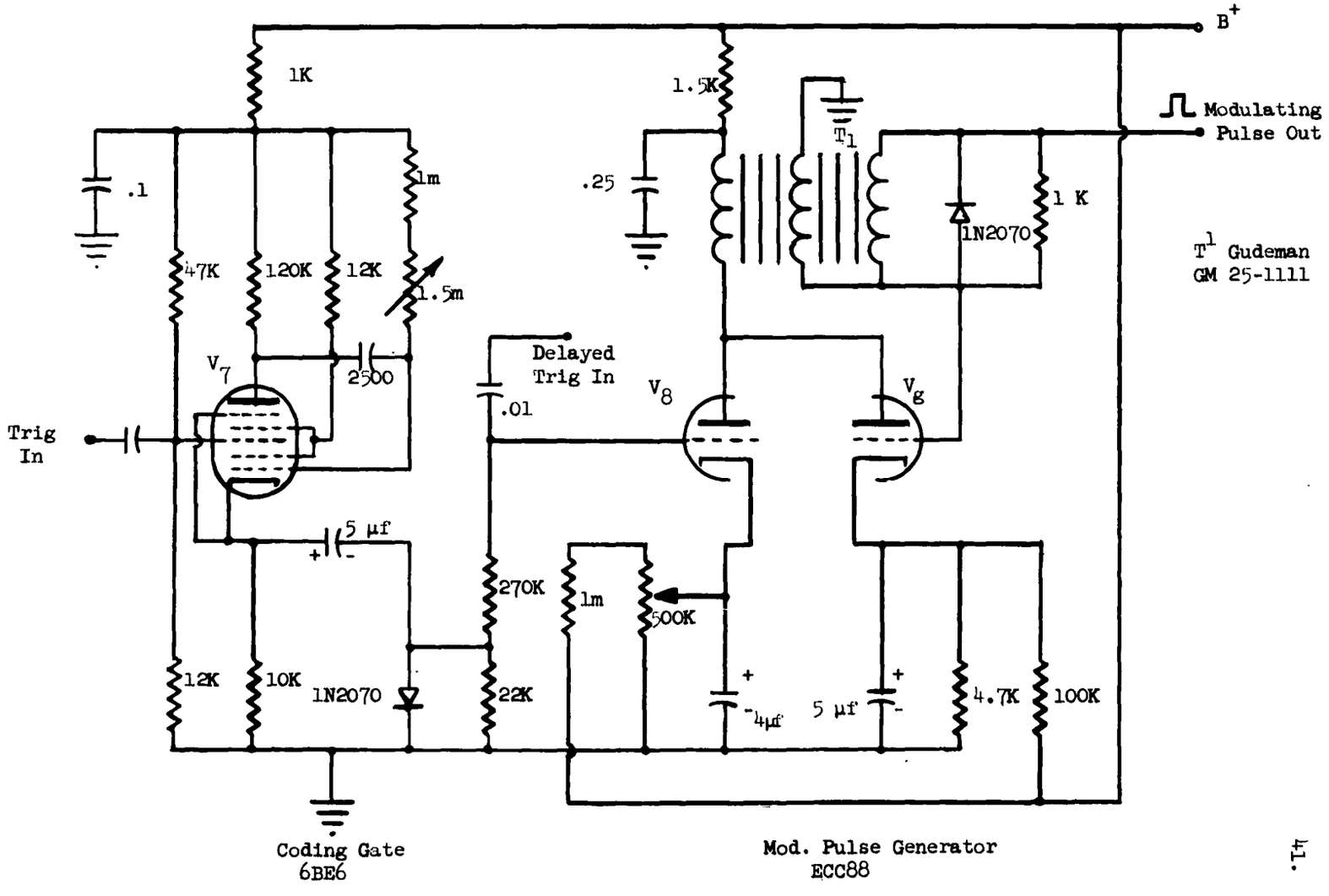

Fig. 15. Coding Gate and Pulse Generator

the tube beyond cutoff for the incoming triggers and blanking the output during this time interval. A variable cathode bias on V_8 provides an adjustable clipping level to insure proper pulse coding. A two to one voltage step-up in the output transformer gives a 300 volt modulating pulse, which is approximately 15 μs long.

D. Oscillator. The oscillator circuit is shown in Fig. 16. It is essentially a modified tuned grid tuned plate oscillator capable of crystal or varicap* modulation control, depending on the position of switch S_1. In the varicap modulated position, the staircase waveform is applied as a back bias voltage on similar pairs of varicaps in the grid and plate circuits so that the resonant frequencies of their respective tuned circuits vary approximately together, thus varying the output frequency as a function of step voltage. One disadvantage of this type of modulation is that the output frequency is not a linear function of the bias voltage. The varicap characteristic curve of Fig. 17 shows that the capacitance varies roughly as the reciprocal square of the bias voltage. The resultant change of oscillator frequency with bias voltage is shown in Fig. 18. Although oscillator linearity is not a requirement of the system, it is a desirable feature and Fig. 18 indicates that the oscillator does exhibit a fair degree of linearity over a one megacycle band. With the switch in the crystal controlled position, the resonant frequency of the grid circuit and hence the frequency of oscillation is determined by the parallel resonant frequency of the crystal.

---

*Pacific semi-conductors Inc. Voltage variable capacitor.

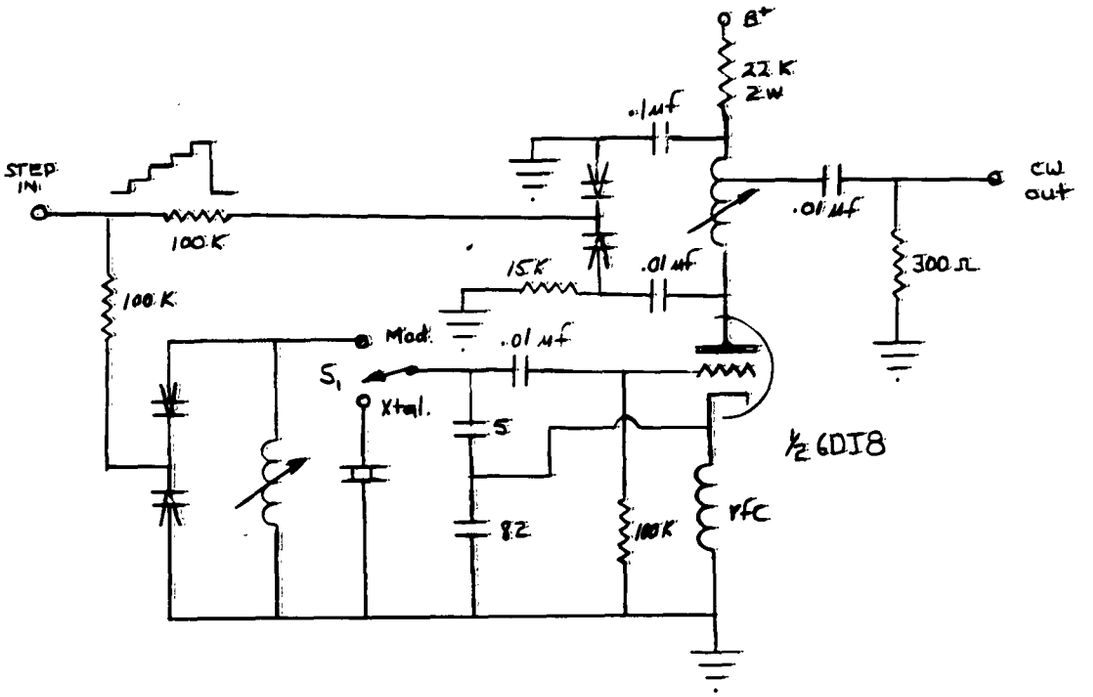

Figure 16. OSCILLATOR

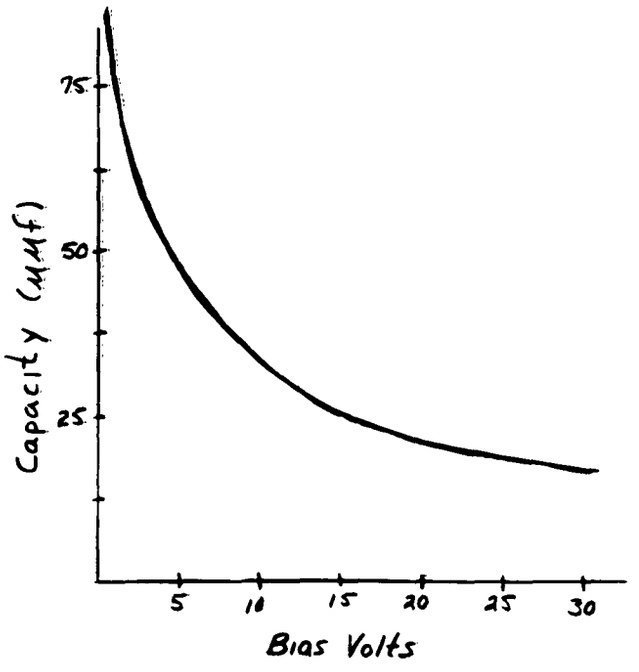

Figure 17. VARICAP CHARACTERISTICS

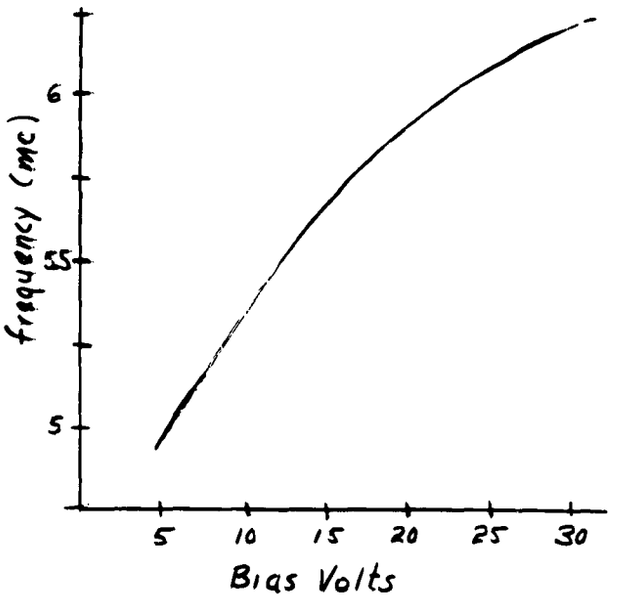

Figure 18. OSCILLATOR CHARACTERISTICS

The oscillator output is taken from a low impedance tap point in the plate circuit. The impedance level was selected for a nominal plate circuit Q of about 5 over the operating range to preserve the wave shape. Taking the output from the plate circuit also prevents any appreciable loading in the grid circuit and allows more stable operation. The cw output is approximately 1 volt peak with an output impedance of 300 ohms.

E. Amplifier Investigation. Several methods of approach were investigated before deciding how the amplifier stages of the transmitter could be designed to best meet the requirements. The transmitter specifications require a one megacycle bandwidth at any center frequency in the operating range.

1. Tuned Amplifier Stages. The simplest method of obtaining the required amplification at any given center frequency is by use of tuned rf stages with the Q of the circuits adjusted to give the required bandwidth. Variable inductive or capacitive tuning could be used to vary the center frequency over a small range. For a fixed coil or capacitor however, the bandwidth of the stage is a function of the center frequency to which the stage is tuned, and in general the impedance match between stages will also depend on the center frequency. These problems could be overcome by using a combination of inductive and capacitive tuning, but retuning procedures would indeed be quite difficult and very time consuming. These limitations would indicate that the only practical method of covering the required four to one frequency range using tuned amplifier stages would be by the use of "plug-in" tuned circuits for each stage, each covering about a one megacycle range. This would require a minimum of

seven or eight plug-in units for each tuned circuit.

2. Transformer coupled stages. The possibility of using transformer coupling in conjunction with video peaking techniques was also considered. Class A operation in the power stages of the transmitter is impossible at the required power levels and hence, push-pull Class B operation would be required to maintain the rf waveform after the low level class A stages. The broad band transformers for use in this application would be required to operate at relatively high impedance levels over a frequency range of 4 mc to 12 mc. Various transformer winding techniques were investigated mostly using toroid cores of ferrite material. Attempts to make a phase inversion or balanced-to-unbalanced transformer for use over this frequency range indicated that without the use of special techniques, the impedance level of such transformers was limited to the neighborhood of 200 ohms by shunt capacitances and leakage reactance. Also, with ferrite transformers there exists the problems of core saturation in the high level stages.

3. Distributive Amplification. The use of distributive amplification would completely eliminate the need for tuning and render the system inherently broad-band. The same problems in preservation of the rf waveform in the high level stages exists here as in the transformer coupled design; class B push-pull operation would be required. Another problem to be considered is that no appreciable grid power can be drawn by the individual tubes in a distributed amplifier or the grid line becomes lossy and operation is seriously impaired. Also, one half of the rf power in the plate circuit of a distributed stage is absorbed in the reverse line termination leaving only one half available for the load. These limitations would make distributive techniques impractical for the

rinal power stages where considerable grid drive is required for efficient operation; but in the low level stages, these objections are not serious.

F. Low Level Distributed Amplifier. On the basis of the above investigation, it was decided to use a distributed amplifier to supply enough gain to the cw oscillator signal to allow the use of convenient pulse modulation techniques. A suitable level was selected as 25 volts. For an input signal of .5 volts, the required over-all voltage gain is 50. The Amperex E 180F/6688 pentode was selected as the amplifier tube because of its high transconductance. For a distributed amplifier stage, the reference voltage gain is:

$$A = N \frac{g_m Z_{op}}{2}$$

N = No. of tubes
g_m = transconductance
Z_{op} = characteristic impedance of plate line.

for the 6688 $g_m = 16{,}500\ \mu\mho$

Therefore

$$A = N \times 8.25 \times 10^{-3} Z_{op}$$

The voltage gain is directly proportional to the characteristic impedance of the plate line. Therefore, it is desirable that this impedance be as high as possible to achieve the gain with a minimum number of tubes. In this application, we need not be concerned with the phase response of the transmission lines and therefore, constant k filter sections may be used.

For a single low pass T section

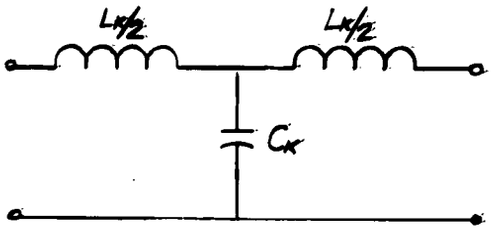

The characteristic impedance is

$$Z_o = \sqrt{\frac{L_k}{C_k}} \qquad (1)$$

and the cutoff frequency is

$$f_c = \frac{1}{\pi \sqrt{L_k C_k}} \qquad (2)$$

Combining these two equations yields:

$$Z_o = \frac{1}{\pi f_c C_k}$$

Therefore, the highest characteristic impedance which can be obtained for a given cutoff frequency is when the shunt capacitance is a minimum. The output capacitance of the 6688 is approximately 3 μμf. Stray wiring capacitance per stage was estimated at 3 μμf giving a minimum relizable capacitance per section of 6 μμf. If a cutoff frequency of 20 mc is required, the highest possible characteristic impedance is

$$Z_o = \frac{1}{\pi \times 20 \times 10^6 \times 6 \times 10^{-12}} = 2650\ \Omega$$

giving a maximum gain per state of

$$A_{\infty} = 8.25 \times 10^{-3} \times 2.65 \times 10^{3} \approx 22$$

It was discovered, however, that in this impedance range, ordinary carbon resistors do not exhibit a pure resistance at frequencies above a few megacycles and hence, do not provide proper termination to the transmission line. A 1.5 k carbon resistor was found to have a phase angle in the order of -30° at 15 mc and thus was chosen as the upper limit on the terminating impedance for the line. For $Z_{\infty} = 1.5k$, then the gain per stage is

$$A_{\infty} = 8.25 \times 10^{-3} \times 1.5 \times 10^{3} = 12.4$$

for an overall gain of 50

$$50 = 12.4\ N$$

$$N \approx 4$$

Four stages are required.

1. Plate circuit transmission line. The plate circuit transmission line requires four constant k low pass T filter sections to be cascaded. M - derived terminating half sections with m = .6 should be used to supply the best possible match between the line and the terminating impedance over the pass band. Combining equations (1) and (2), we get the necessary design equations.

$$C_k = \frac{1}{\pi f_c R_o} \qquad (3)$$

$$L_k = R_o^2 C_k \qquad (4)$$

For $Z_{op} = 1500$ and $f_c = 20$ mc

$$C_k = \frac{1}{\pi \times 20 \times 10^6 \times 1500} = 10.6 \ \mu\mu f$$

$$L_k = (1500)^2 \times 10.6 \times 10^{-12} = 23.8 \ \mu h$$

Terminating half sections $m = .6$

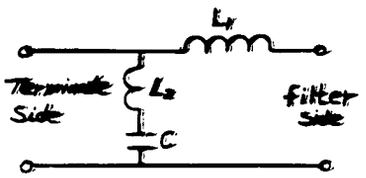

$$L_1 = \frac{m}{2} L_k = .3 \times 23.8 = 7.15 \ \mu h$$

$$L_2 = \frac{1-m^2}{2m} L_k = .533 \times 23.8 = 12.7 \ \mu h$$

$$C = \frac{m}{2} C_k = .3 \times 10.6 = 3.5 \ \mu\mu f$$

The complete 4 section plate line is shown in Fig. 19. In the amplifier

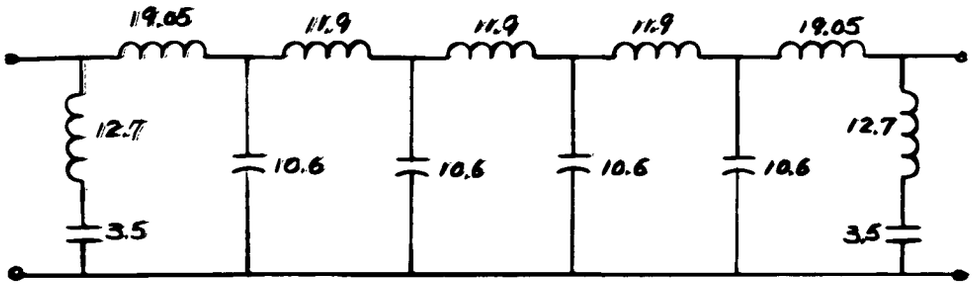

All inductors in the μh
All capacitors in μμf

Fig. 19. Plate circuit transmission line

circuit, the output capacitance of each tube and the stray wiring capacitances will be absorbed in the shunt capacitors. For the 6688 the output capacitance is approximately 3 μμf. Stray wiring capacitance per stage was estimated at 2 to 3 μμf per section; thus an additional 5 μμf was added in parallel with the output capacitance of each tube.

2. Grid Circuit Transmission Line. The design of the grid circuit line is restricted to the condition that the propagation constant at all frequencies be identical with that of the plate line. This condition is satisfied if the cutoff frequency is made the same as that of the plate line. The input impedance of the amplifier was chosen as 250Ω to match the oscillator output. Using the design equations (3) and (4).

$$C_k = \frac{1}{\pi \times 20 \times 10^6 \times 250} = 63.6\ \mu\mu f$$

$$L_k = (250)^2 \times 63.6 \times 10^{-12} = 3.98\ \mu h$$

Terminating half sections $m = .6$

$$L_1 = \frac{m}{2} L_k = .3 \times 3.98 = 1.2\ \mu h$$

$$L_2 = \frac{1-m^2}{2m} L_k = .533 \times 3.98 = 2.12\ \mu h$$

$$C = \frac{m}{2} C_k = .3 \times 63.6 = 19.1\ \mu\mu f$$

The complete grid line is shown in Fig. 20. The input capacitance of each tube is 10 μμf and allowing approximately 4 μμf stray capacitance per stage , an additional 50 μμf must be added in parallel with the grid of each tube. The complete distributed amplifier is shown in Fig. 21.

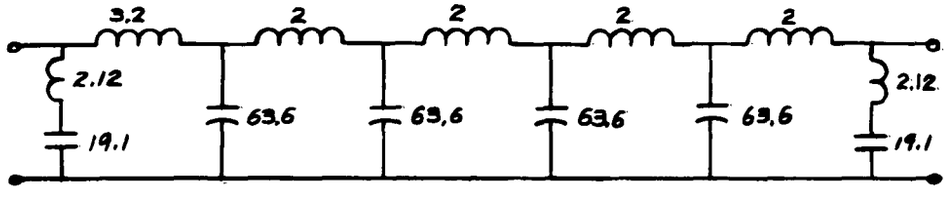

All inductors in μh
All capacitors in μμf

Fig. 20. Grid Circuit Transmission Line

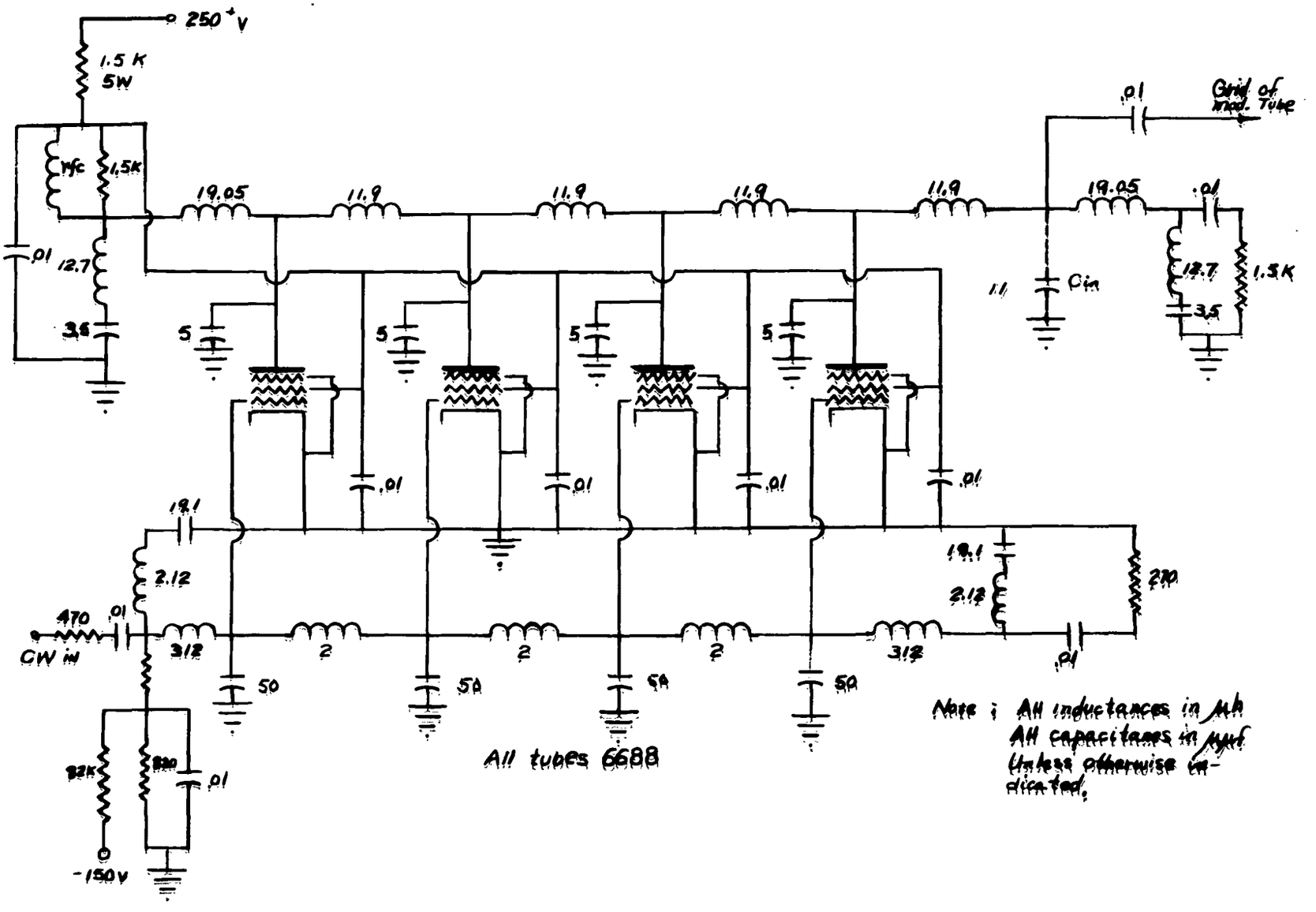

Figure 21. LOW LEVEL DISTRIBUTED AMPLIFIER

G. Pulse Modulator. The rf amplification thus far is broad band and yields essentially constant output over the required frequency range. It is highly desirable that the pulse modulation also be accomplished without the use of tuned circuits and their inherent limitations and disadvantages as discussed earlier. Another problem is that the lower operating frequencies are not well removed from the significant components of the modulating pulse and isolation of the video pulse is quite difficult. Both of these problems are overcome by the circuit of Fig. 22. A secondary emission pentode is used as a balanced modulator. The modulating pulse from the 15 μs pulse generator is applied to the screen grid allowing the tube to be operated in a zero bias state. The cw input to the grid is taken directly from an additional filter section in the plate line of the

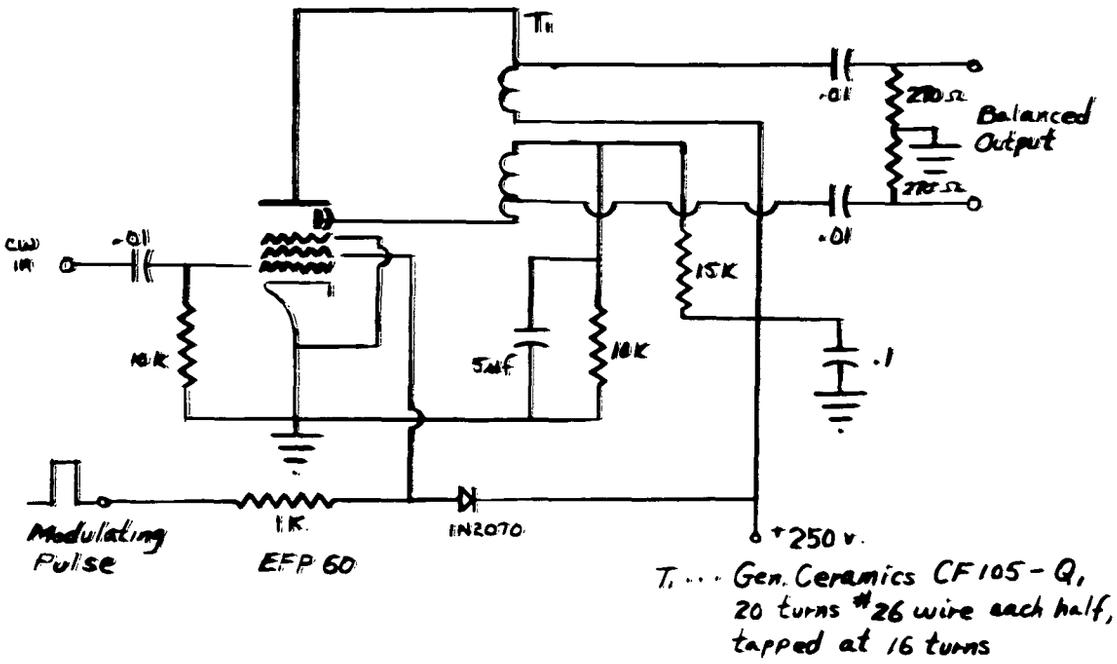

Figure 22. PULSE MODULATOR

distributed amplifier thereby eliminating the necessity of a tuned circuit or matching transformer. The output is a balanced load connected between the plate and the secondary emission cathode by means of a ferrite core inductor. The secondary emission cathode and plate current components resulting from the modulating pulse are effectively cancelled out in the ferrite core giving only the rf pulse across the balanced load.

H. Power Amplifier. In order to estimate roughly the maximum power which should be required from the transmitter, the receiving antenna was assumed to be a linear dipole approximately one half wave length long.

For a linear half wave dipole, the maximum effective aperture is[9]

$$A_{e\ max} = .13\lambda^2 = \frac{(V_{in})^2}{R_r P_r}$$

V_{in} = voltage across receiver input

R_r = radiation resistance of the Antenna

P_r = power density of incoming signal

If the antenna has a finite loss resistance, the effective aperture is:

$$A_e = K A_{e\ max} \quad \text{where} \quad K = \frac{R_r}{R_t}$$

R_t = termination resistance

---

[9]Kraus, "Antennas", McGraw Hill Book Co., Inc. New York, New York, p. 51; 1950

A study of low frequency dipole antennas for use on rockets has been made[10] and results indicate that a minimum expected efficiency would be somewhat greater than 30. Thus, if we assume an antenna efficiency of 10%, this should also allow for a slight mismatch on the antenna should it occur and also provide reception over most of the dipole antenna pattern. The effective aperature should then be in the order of:

$$A_e = .1 \times .13 \lambda^2 = 1.3 \times 10^{-2} \lambda^2 = \frac{(V_{in})^2}{R_t P_r}$$

but

$$P_r = G_1 \frac{W}{4\pi h^2}$$

W = transmitter output power

G_1 = Ground ant. gain

h = rocket altitude.

$$P_r = \frac{(V_{in})^2}{1.3 \times 10^{-2} \lambda^2 R_t} = \frac{G_1 W}{4\pi h^2} \qquad (4)$$

$$W = \frac{4\pi}{1.3 \times 10^{-2} G_1 R_t} \left(\frac{h}{\lambda}\right)^2 (V_{in})^2 \qquad (5)$$

Antenna investigations indicate R_t should be approximately 25 ohms for the type of antennas to be used.[11] Past experience indicates that under extreme conditions, it may be necessary to have an input voltage to the receiver in the order of 200 μ volts to overcome the ambient noise level

---

[10] Miner, op. cit.

[11] Miner, op. cit., p. 41

in this range of operating frequencies. If we therefore require V_{in} = 200 μ volts for the minimum frequency of 4 megacycles and require operation to an altitude of 1000 kilometers:

$$\lambda = 25 \text{ meters} \quad \frac{h}{\lambda} = \frac{1x10^6}{25} = 4x10^4$$

If the plasma frequency at any position in the rocket trajectory approaches relatively close to the operating frequency, high signal attenuation may result. To make allowance for some attenuation as well as the losses in the transmitting antenna, we might assume the transmitting antenna to have an effective gain of G_1 = .1. The required power then is roughly

$$P = \frac{4\pi}{1.3x10^{-2} x .1x25} \quad (x\ 16x10^8\ x)(4x10^{-8}) \text{ watts}$$

$$= 386 \times 16 \times 4 = 24 \text{ KW}$$

Realizing that this should represent the extreme case, it was felt that a peak power output of 20 KW would constitute a very conservative design.

The design details resulting in the complete power amplifier of Fig. 23 will now be examined.

1. Output stage. The design of the power amplifier was carried out in the usual manner once the required output power was determined. The first step was the design of the output stage.

The 4CN15 ceramic tetrode was chosen as the output tube because of its small physical size and high pulse power capabilities. It was determined that 10 KW could be obtained if the tube was operated class B with 1000 volts on the screen grid and 7000 volts on the plate. Thus, two tubes

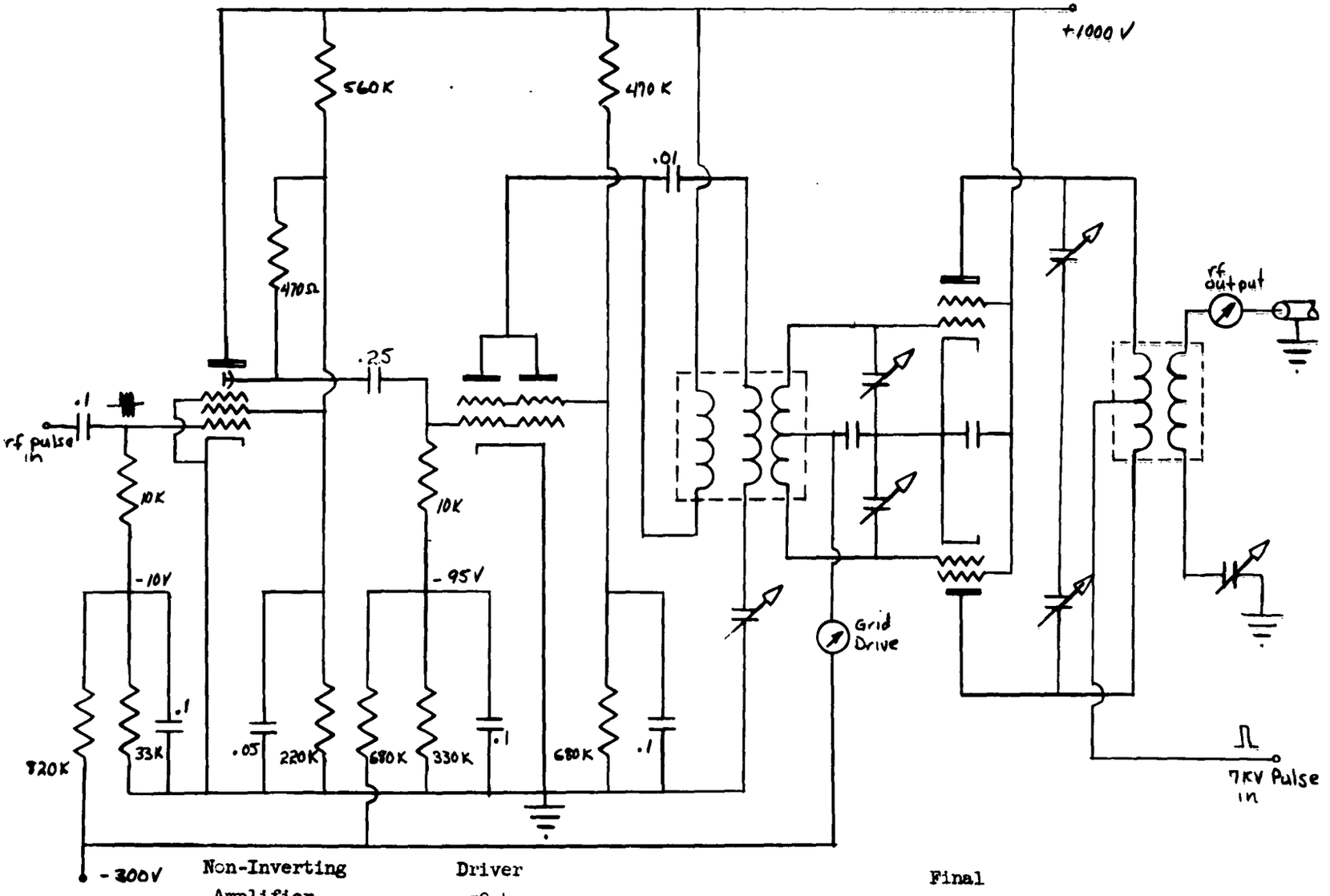

Figure 23. POWER AMPLIFIER

were needed to produce the required power. The class B design of the output stage is included in Appendix II. In order to stay within the voltage ratings of the tubes, it was necessary that the plate supply be pulsed. For this reason, it was decided that the output stage would be both grid and plate modulated. This was accomplished by making the grid pulse considerably longer than the desired output pulse and allowing the plate pulse to control the pulse width. A grid pulse of 15 μ sec duration was used with a plate pulse of 5 μsec being triggered approximately 5 μs after the start of the grid pulse. This eliminates all rise-time and transient effects from the grid pulse.

The primary problem in the plate modulation of the output stage is that the lower portion of the operating frequency range is not well removed from the significant components of the modulating pulse and isolation becomes difficult. This problem can be overcome by operating the output tubes in push-pull and feeding the modulating pulse on the center tap of the balanced output transformer. Because of the difficulties, discussed earlier, in winding broad-band magnetic core transformers of the balanced to unbalanced type, it was decided that it would be necessary to tune the output circuit to match the plate to plate impedance to 50 ohms. Saturation problems in magnetic core materials made it more desirable to use fixed air core inductors with variable capacitance tuning. Push-pull class B operation of the output tubes allows the use of relatively low Q circuits without serious distortion of the rf waveform. The tuned circuit was constructed such that "plug-in" coils could be used to extend the tuning range from 4 mc to 12 mc. The range of tuning

achieved with each coil was governed primarily by the capacitance range of the variable capacitors and by the usable range of circuit Q which was allowed.

The plate to plate impedance of the output stage was matched to 50 ohms by the use of series tuning in the secondary and a parallel tuned primary. For this configuration, the load resistance R_2 is reflected as an equivalent resistance in series with L_1 according to the relationship for critical coupling:

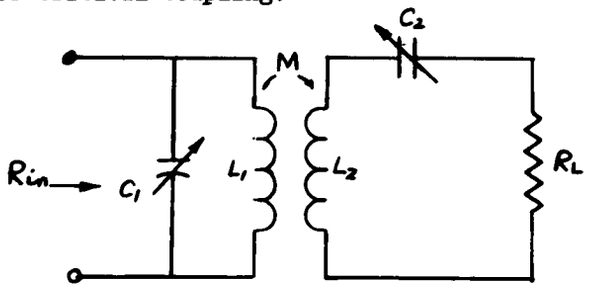

$$X_m \text{ critical} = \sqrt{R_1 R_L}$$

$$R_1 = \frac{X_m^2}{R_L}$$

where $X_m = \omega M$

R_1 = equivalent resistance in series with L_1

The equivalent parallel primary resistance is

$$R_{(par)} = \frac{(\omega L_1)^2}{R_1} = R_{in}$$

$$R_{in} = \frac{\omega^2 L_1^2}{\omega^2 M^2 / R_1} = \left(\frac{L_1}{M}\right)^2 R_1$$

This result indicates that the impedance match for this configuration is independent of frequency, and therefore will not limit the usable tuning range of the circuit. In order to obtain the maximum tuning range with variable capacitors which were physically small enough to be used in the unit, the Q of the primary was allowed to be quite low. The bandwidth

of the circuit was then determined by the secondary Q which was allowed to vary approximately between 5 and 10 over the tuning range. The required frequency range was covered with two plug-in coils and variable capacitance tuning.

2. Driver Stage. The output stage requires a drive signal of 800 volts peak across an equivalent grid to grid impedance of 1230 Ω, or an input power of 260 watts which must be supplied by the driver stage.

A 5894 beam power dual tetrode was used for the driver. The class "C" design is included in Appendix II. The two halves of the tube were operated in parallel with 1000 volts on the plate and a screen potential of 600 volts. There was some doubt as to the accuracy of the required drive power in the output stage design because the published characteristic curves had to be transformed for a higher screen voltage. Therefore, a conservative approach was taken and the drive design which was used gave a total of 380 watts for the two halves of the tube in parallel. The plate impedance of the driver was matched to the final stage by a second tuned circuit. The same series-parallel tuning configuration which was used in the output circuit was again employed so that the impedance match would not vary with frequency. This required that the driver be shunt fed to allow series tuning in the plate circuit and parallel tuning in the secondary to supply the balanced push-pull grid circuit of the final. By allowing the Q of the parallel tuned secondary to be quite low, a greater tuning range was possible for the variation in capacitance which was available. The bandwidth was then determined by the series tuned primary, as was the case in the output circuit, by allowing a

variation of circuit Q approximately between 5 and 10. The required frequency range was covered in a series of three plug-in coils.

3. Non-Inverting Intermediate Amplifier. The design of the driver in Appendix II indicates that the pre-drive stage must supply 110 volts peak rf during the pulse. In the interest of simplicity, it was desirable that this be accomplished without the use of any additional tuned circuits. Due to the high input capacity of the driver stage, a resistance-coupled amplifier designed to cover the required frequency range must employ a tube with a high figure of merit in order to achieve a reasonable gain. A conventional resistance-coupled amplifier, however, would be required to operate class "A" to produce a positive output for the following stage, or a broad-band inversion transformer would have to be used. Both of these alternatives present serious problems. It was decided that these problems could be eliminated by using a secondary emission pentode as a non-inverting amplifier, taking the output from the secondary emission cathode as shown in Fig. 23. This tube has an extremely high figure of merit when operated near the zero bias region and provided the necessary gain between the output of the pulse modulator and the driver stage.

I. The High Voltage Pulsed Power Supply. The remaining problem in the power amplifier design is a power supply to produce the 7 KV 5 μsec plate pulse for the output stage. The method used to produce the pulse was the discharge of a pulse-forming network throughout a hydrogen thyratron. The complete high voltage power supply is shown in Fig. 24. This power supply also produces 1000 volts d.c. which is used in the remainder of the power amplifier.

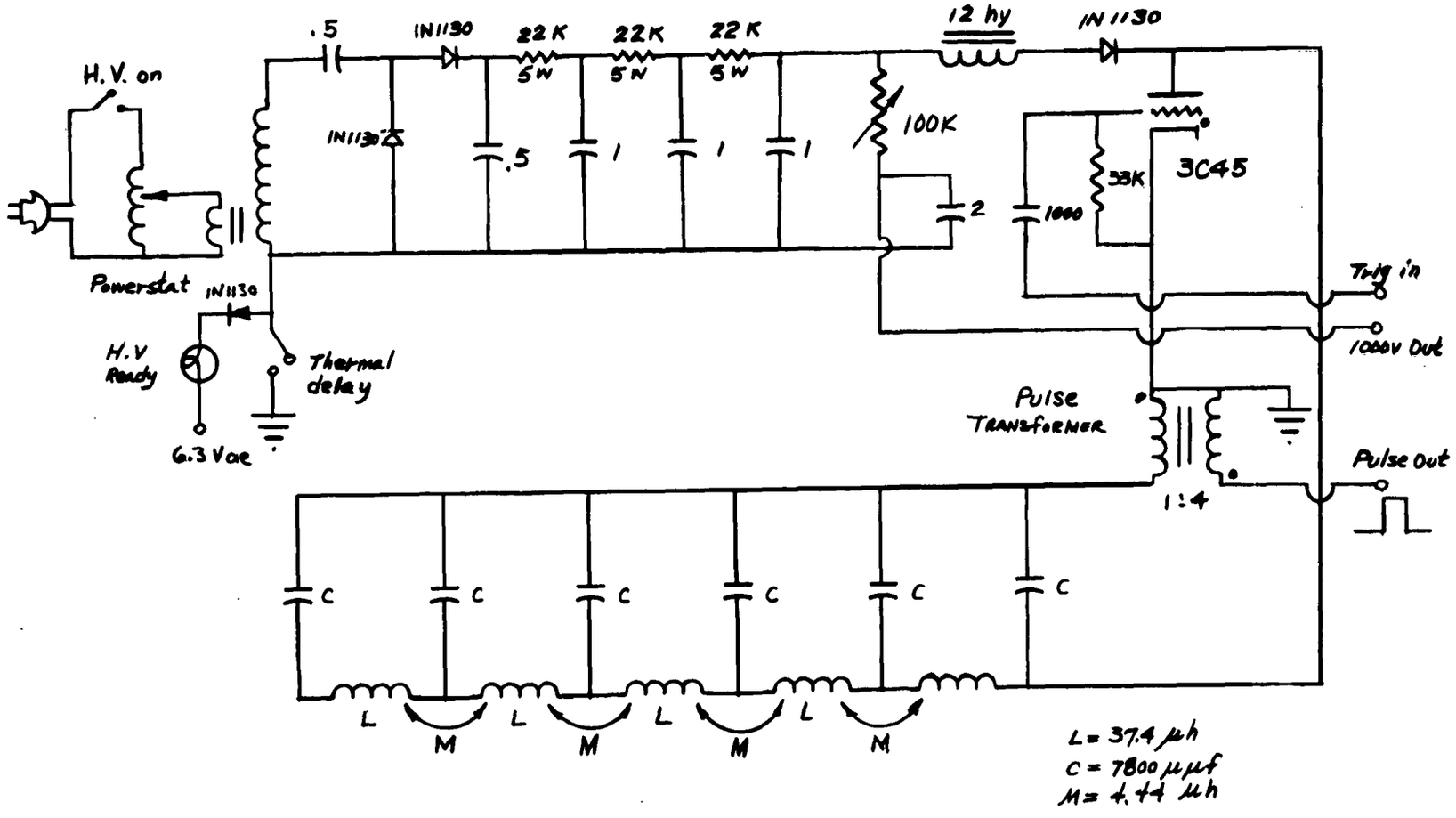

Figure 24. HIGH VOLTAGE PULSE POWER SUPPLY

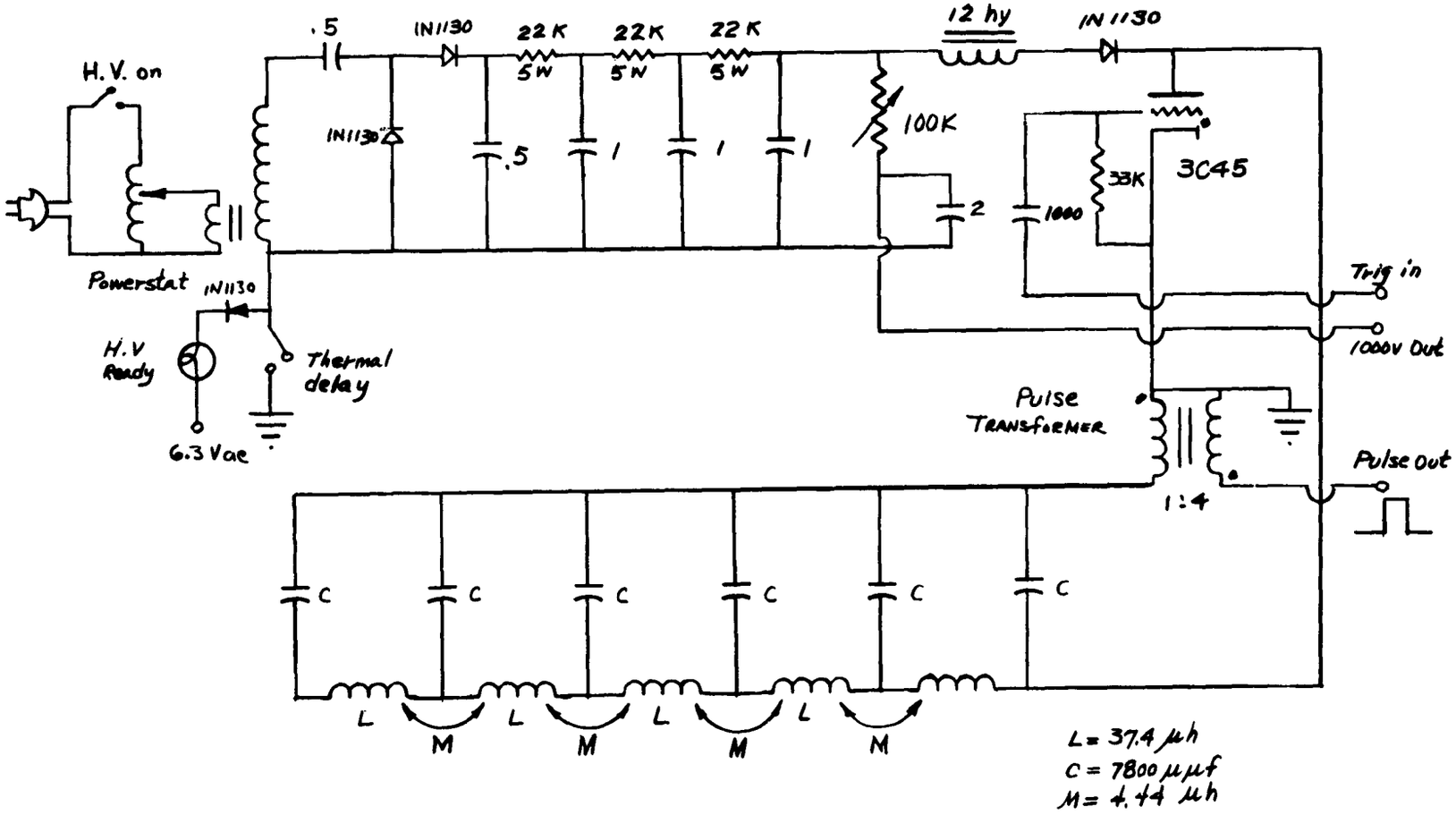

Figure 24. HIGH VOLTAGE PULSE POWER SUPPLY

1. The Pulse-forming Network. A five section m-derived delay line was used as the pulse-forming network. The optimum condition for constant delay per section as a function of frequency over the pass-band is obtained with m=1.27[12]. In terms of the resultant pulse, this gives the best compromise between rise-time and overshoot. To find the required characteristic impedance of the line the desired output power and voltage had to be determined. For reasons which will be discussed later, it was decided that a 4:1 step-up ratio was approximately the upper limit for a pulse transformer which could be used to boost the output pulse voltage in this application. Since the output stage of the power amplifier has an efficiency of approximately 50%, the power supply must produce a 7000 volt, 40 KW pulse. For a 4:1 step-up ratio, the line discharge voltage must be 1750 volts and the characteristic impedance of the line is

$$Z_o = \frac{V^2}{P} = \frac{(1750)^2}{40\times10^3} = 76.5\ \Omega$$

The delay to rise time ratio for an m-derived filter with m=1.27 is found to follow the relationship [13]

$$\left(\frac{t_d}{t_r}\right)^{1.5} = \frac{n}{.94}$$

where t_d = total delay time
t_r = rise time
n = number of sections

---

[12] Millman and Taub, op. cit. p. 295

[13] Ibid., p. 297

If we require a pulse width of 5 μsec and a rise time of 1 μsec, the required number of sections is:

$$n = .94(5)^{1.5} = .94 \times 11.2 = 10.25$$

For a pulse-forming network consisting of an open-circuit line, the required number of sections is one-half of this or

$$n = 5 \text{ sections}$$

To complete the design of the pulse-forming network, the following expressions are used to determine the values of a constand k low pass T section.

$$\text{delay per section} \quad t_s = 1.27\sqrt{L_k C_k}$$

$$\text{characteristic Impedance} \quad Z_o = \sqrt{L_k/C_k}$$

to allow for the rise time of the circuit, let $T_s = .6$ μ sec.
Then for $Z_o = 76.5\,\Omega$

$$76.5 = \sqrt{L_k/C_k} \qquad L_k = (76.5)^2 C_k$$

and

$$.6\text{x}10^{-6} = 1.27\sqrt{(76.5)^2 C_k^2} = 1.27 \times 76.5\, C_k$$

$$C_k = .0062\ \mu\text{f}$$

$$L_k = (76.5)^2 \times 6.2\text{x}10^{-9} = 36.3\mu\text{h}$$

For an m-derived low pass T filter section of standard configuration, the inductance in the center arm becomes negative for m greater than one. This

can be rectified by using the following equivalent network which utilizes mutual coupling between the two series arms.

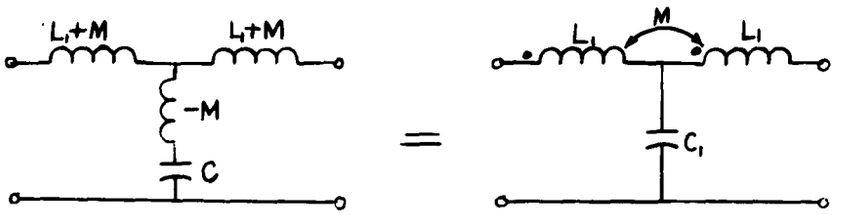

where $L_1 + M = \frac{m}{2} L_k$

$-M = \frac{1-m^2}{4m} L_k$

$C_1 = m\, C_k$

Therefore, the design equations for L_1 and C_1 in terms of L_k and C_k are:

$$L_1 = \frac{m^2+1}{4m} L_k \qquad C_1 = m\, C_k$$

And for this case the required values are:

$$L_1 = \frac{(1.27)^2+1}{4\times 1.27} \times 36.3 = .515 \times 36.3 = 18.7\ \mu h$$

$$M = \frac{(1.27)^2 - 1}{4 \times 1.27} \times 36.3 = .1.22 \times 36.3 = 4.44\ \mu h$$

$$C = 1.27 \times .006\ 2 = .0087\ \mu f$$

The complete five section line is included in Fig. 24.

2. Output Pulse Transformer. The four to one pulse transformer was would on a high permeability ferrite torroid. By knowing the required voltage and pulse width and the characteristics of the core material, the required number of turns to avoid saturation was determined from the relationship

$$N = \frac{V}{\Phi_{max}} \Delta t$$

V = pulse voltage

Φ max. = maximum allowable flux in the core

Δt = pulse interval

which can easily be derived from the basic equation.

$$V = -N \frac{d\phi}{dt}$$

A core was selected which allowed the required number of secondary turns to be wound in no more than two layers in order that the shunt capacity between layers be kept to a minimum. Since the transformer must invert the pulse as well as provide a four-to-one voltage step-up, it was necessary that shunt capacity between the primary and secondary windings be kept to a minimum also, while at the same time obtaining the maximum possible magnetic coupling. Experimentation led to the conclusion that the maximum usable step-up ratio for this application was approximately four-to-one. The increasing shunt capacitances and leakage reactance at higher ratios began to seriously distort the pulse shape.

3. D.C. Supply and Charging Circuit. The pulse forming delay line is charged through an inductor and diode in series with the d.c. supply. The inductor was so chosen that it resonates with the total capacitance of the delay line at a frequency somewhat higher than the maximum expected operating P.R.F. Immediately after the discharge of the delay line, the series resonance of the inductor and delay line capacitance causes a sinusodial charging current to flow. Since the voltage across the capacitor lags the

current by 90°, the voltage starts at a minimum point of the sinusoid and charging continues for one-half cycle until the peak of the wave form is reached. The series diode then clamps the voltage to this point. This method has a great advantage over conventional series resistance charging in that the line is charged to essentially twice the supply voltage without dissipation of power.

To supply a discharge pulse of 1750 volts, the line must be charged to twice this value. Since the supply voltage is doubled by the resonant charging circuit, the d.c. power supply must produce 1750 volts. This is supplied by a 1000 volt transformer in conjunction with a standard voltage doubler and an RC filter. A thermal delay relay was incorporated to allow the power amplifier tubes a minimum warm-up time of sixty seconds before application of the high voltage.

VII. SUMMARY AND CONCLUSIONS

The upward pulse delay system which has been described, is capable of measuring the vertical distribution of the free electron density of the Ionosphere. Small scale variations in the horizontal distribution can also be obtained by extending the system to include several low frequency transmitters. By using large separation of the transmitters on the ground, multiple paths to the rocket are obtained. The data recorded for the various paths then gives an indication of the horizontal structure of the Ionosphere. The use of multiple transmitters requires the addition of a time sychronization system so that the different transmitters can be pulsed in proper time sequence.

The airborne equipment, exclusive of the reference link, consists only of the low frequency receiver and a dipole antenna. The antenna is mounted externally and requires very little internal space. The low frequency receiver occupies a space 5 1/2 inches in diameter and 2 inches high. The complete receiver weighs 1/2 pound and has a total power consumption of $\frac{1}{2}$ watt. These small weight and space requirements make it possible to conduct this experiment concurrently with others on the same rocket. Since the low frequency transmitters are to operate from the ground, no stringent weight and space limitations need be imposed except that a unit be easily portable. It was therefore possible to design the transmitter such that a series of frequencies could be investigated simultaneously during an experiment. The transmitter is capable of stepping frequencies over any one megacycle interval from 4 mc to 12 mc. The operating frequency was made quite easily adjustable over this range. Photographs of the complete low

frequency transmitter are included in Figs. 25 to 28. The unit was constructed to occupy a panel height of 21 inches and has a total weight of 110 pounds. Preliminary tests indicated that the system operates satisfactorily. At the time of completion of this paper, however, the system had not yet been used for an actual rocket flight, and therefore, actual performance information could not be included.

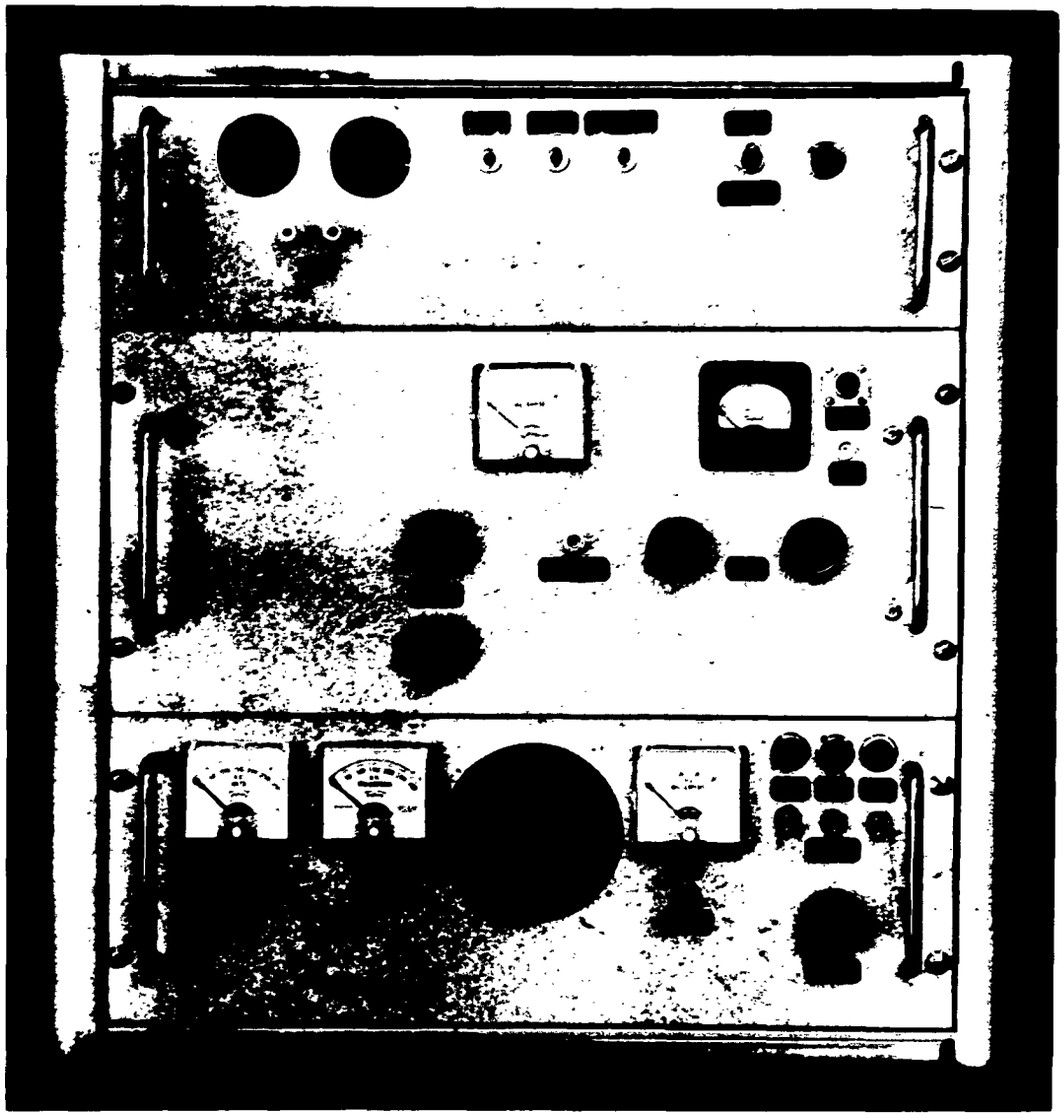

FIGURE 25. UPWARD LOW FREQUENCY TRANSMITTER

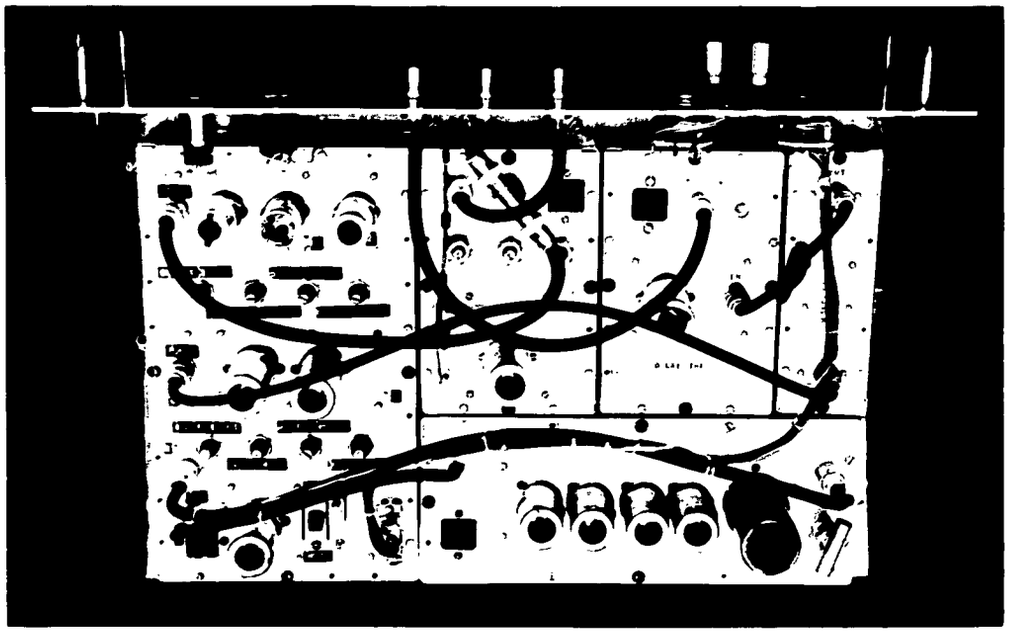

A. Top View

B. Front View

FIGURE 26. LOW LEVEL STAGES

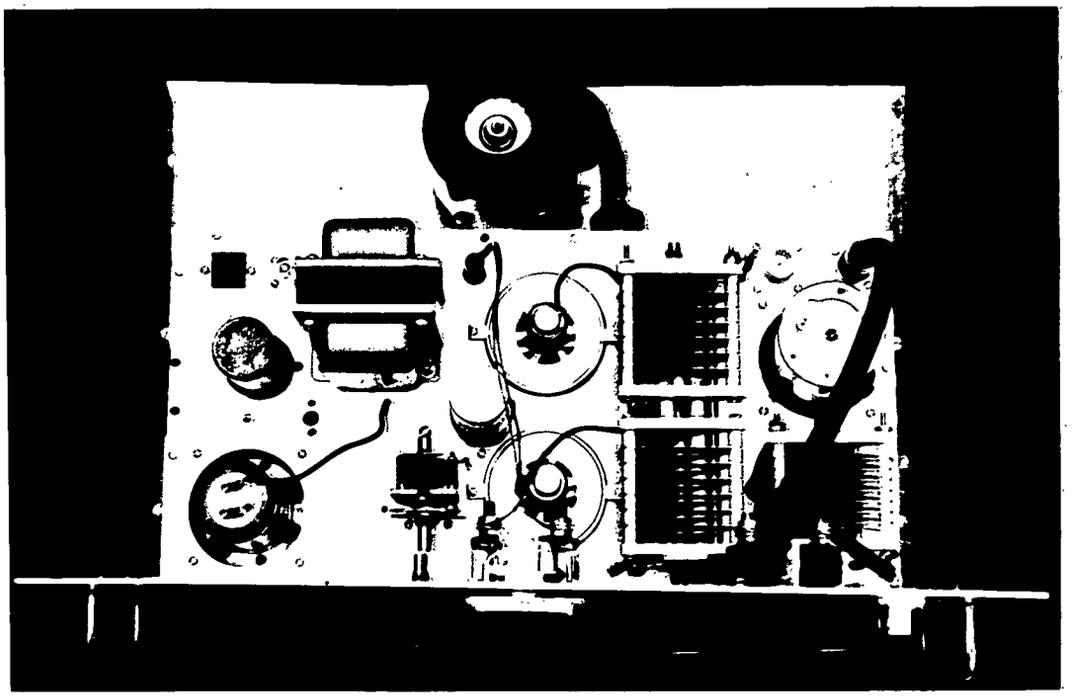

A. Top View

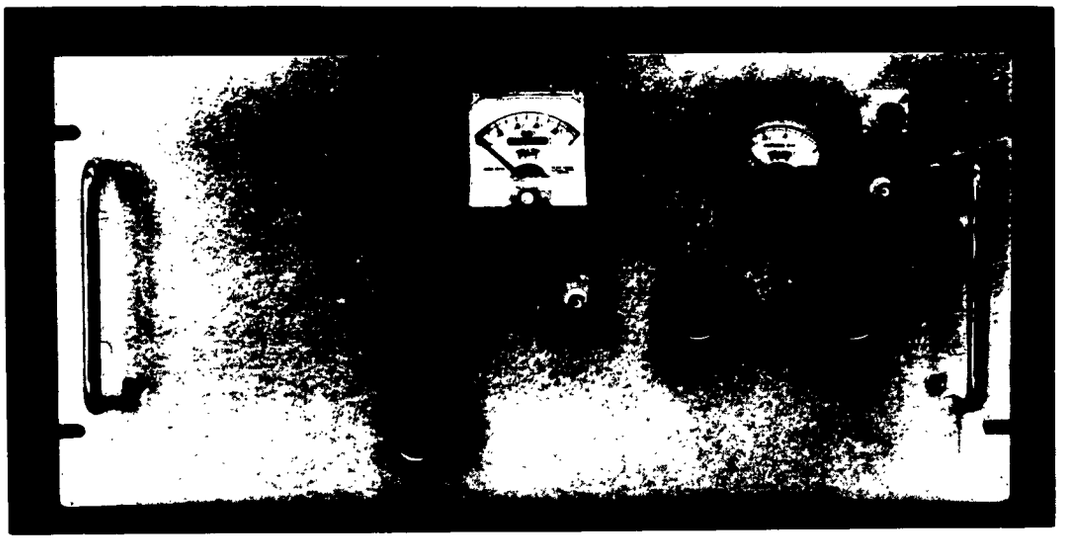

B. Front View

FIGURE 27. POWER AMPLIFIER CHASSIS

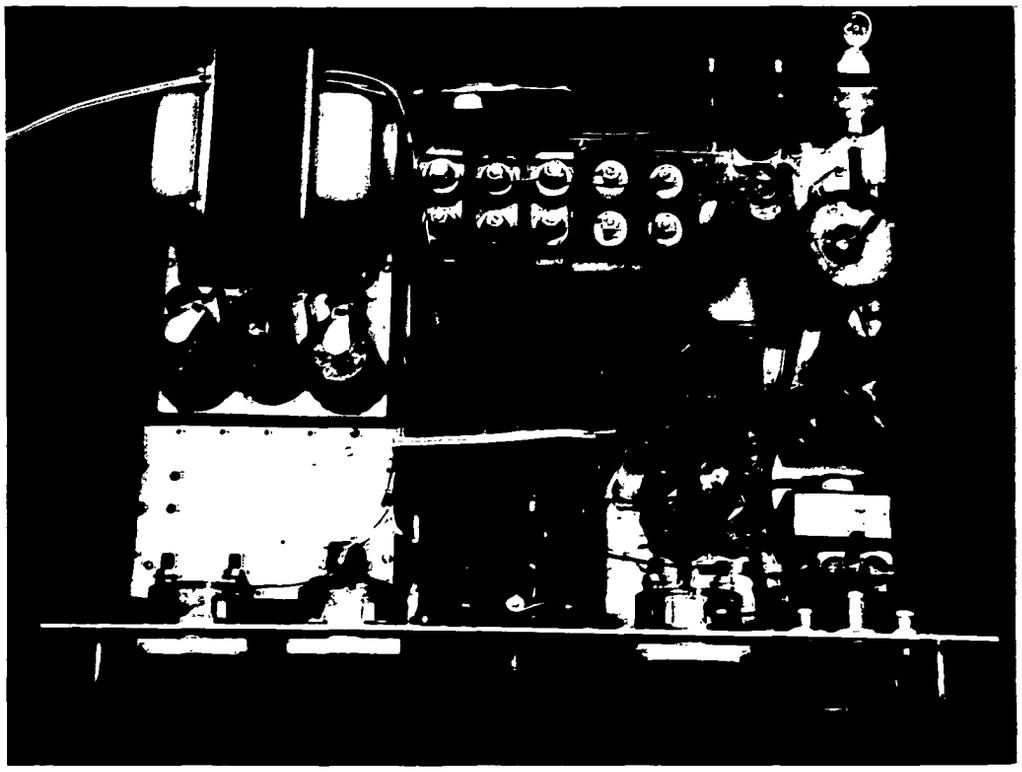

A. Top View

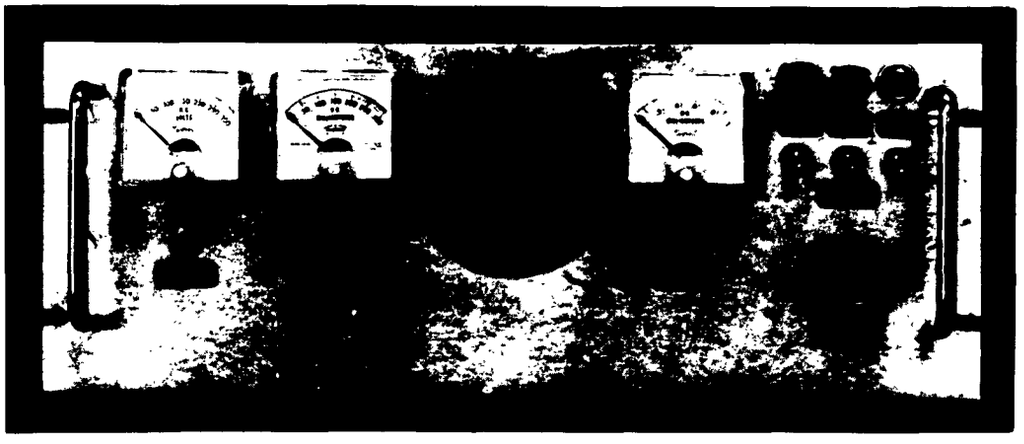

B. Front View

FIGURE 28. POWER SUPPLY CHASSIS

APPENDIX I.

Propagation of Electromagnetic Waves in an Ionized Medium

Consider a linearly polarized plane wave traveling in the positive Z direction.

$$E_x = E_m \sin(\omega t - \beta z)$$

At a given point in space this reduces to

$$E_x = E_m \sin \omega t$$

By Maxwells equation from Amperes law the current is:

$$i = \oint H \cdot dl = \int_s (J + \frac{\partial D}{\partial t}) \cdot ds$$

$$= \int_s \frac{\partial D}{\partial t} \cdot ds + \int_s J \cdot ds = i_{displacement} + i_{conduction} \quad (2)$$

For a lossless dielectric medium the second term is Zero and only the displacement term is present

$$i_d = \int_s \frac{\partial D}{\partial t} \cdot ds = \int_s \varepsilon_0 \frac{\partial E}{\partial t} \cdot ds$$

For a plane wave the Area Vector is in the same direction as E. Hence for a unit area the current is:

$$i_d = \varepsilon_0 \omega E_m \cos \omega t \quad (3)$$

Notice that for the lossless dielectric the current leads the voltage by 90° such that the medium is capacitive in nature.

Now if we assume there are N free electrons per unit volumne in the region which have a collisional frequency ν, we can write the equation of motion of an electron as:

$$eE_x - mv\nu = m \frac{dv}{dt} \quad (4)$$

The first term represents the force on the electron due to the applied field and the second term is the retarding force due to collisions. Rearranging equation (4) into more convenient form and substituting in equation (1) we have:

$$\frac{dv}{dt} + \nu v - \frac{e}{m} E_m \sin \omega t = 0$$

or in Laplace domain

$$v_{(s)} = \frac{eE_m}{m} \omega \frac{1}{(s^2+\omega^2)(s+\nu)}$$

This can then be expanded by partial fractions to yield

$$v_{(s)} = \frac{eE_m}{m(\omega^2+\nu^2)} \omega \left[\frac{-s+\nu}{s^2+\omega^2} + \frac{1}{s+\nu} \right]$$

which can be transformed into the time domain to yield

$$v_{(t)} = \frac{e}{m(\omega^2+\nu^2)} \left[-\omega - j\nu \right] E_m \cos \omega t \qquad (5)$$

The motion of the electron can be interpreted in terms of a resultant current density:

$$J = eNv$$

$$= \frac{Ne^2}{m(\omega^2+\nu^2)} \left[-\omega - j\nu \right] E_m \cos \omega t$$

The conduction current then is:

$$i_j = \int_s J \cdot ds$$

or for a unit area $i_j = J$

The total current then from equation (1) is

$$i = i_d + i_j$$

$$= \left[\varepsilon_0 - \frac{Ne^2}{m(\omega^2+\nu^2)} - j \frac{Ne^2\nu}{m\omega(\omega^2+\nu^2)} \right] \omega E_m \cos \omega t \qquad (6)$$

The bracketed term in equation (6) corresponds to ε_0 for the lossless case of equation (3), and hence it is referred to as the effective dielectric constant of the ionized medium

$$\varepsilon_e = \left[\varepsilon_0 - \frac{Ne^2}{m(\omega^2+\nu^2)} - j\frac{Ne^2\nu}{m\omega(\omega^2+\nu^2)}\right] \tag{7}$$

We can now determine an equivalent circuit for our unit area in the ionized medium by writing the expression for the admittance

$$Y = \frac{\dot{i}}{E} = \frac{\dot{i}}{E_m \sin\omega t} = -\frac{i}{jE_m \cos\omega t}$$

$$= \frac{N_e{}^2\nu}{m(\omega^2+\nu^2)} + j\omega\left[\varepsilon_0 - \frac{Ne^2}{m(\omega^2+\nu^2)}\right]$$

Algebraic manipulation of this expression leads to the following equivalent circuit:

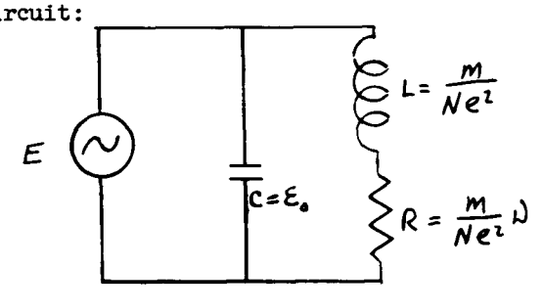

Fig. A.
Equivalent circuit of an Ionized Medium

Thus far we have not taken into account the effects of any external magnetic fields. Therefore in the actual case the derivation must represent a first order approximation in which the earth's magnetic field has been neglected.

The region of interest for the experiment described in this paper is the E layer of the Ionosphere and above, or altitudes from approximately 100 kilometers up. In this region the gas density is so low that the electrons experience a negligible amount of collisions, and the equivalent circuit

of Fig. A. becomes very high Q. For this condition $\Omega \approx 0$ and the effective dielectric constant of equation (7) can be simplified as

$$\varepsilon_e = \varepsilon_o - \frac{Ne^2}{m\omega^2} \tag{8}$$

The effective dielectric constant is thus seen to be less than unity. If we define the plasma or critical frequency of the medium as that frequency at which the dielectric constant becomes Zero then

$$\varepsilon_o = \frac{Ne^2}{m\omega^2} \quad \text{or} \quad \omega_c = \sqrt{\frac{Ne^2}{\varepsilon_o m}} \quad \text{and} \quad f_c = \frac{1}{2\pi}\sqrt{\frac{Ne^2}{\varepsilon_o m}}$$

The effective dielectric constant can then be written

$$\varepsilon_e = \varepsilon_o \left[1 - (f_c/f)^2\right] \tag{9}$$

The physical significance of the effective dielectric constant variation with frequency can be more easily understood by writing the expression for the refractive index of the medium.

$$\eta = \sqrt{\varepsilon_e} = \sqrt{\varepsilon_o\left[1-(f_c/f)^2\right]}$$

For $f = f_c$ the refractive index becomes imaginary indicating that a wave would not propagate in the medium below this frequency, but experience total reflection. For $f > f_c$ the wave will propagate with a phase velocity

$$v_p = \frac{1}{\sqrt{\mu\,\varepsilon_e}} = \frac{1}{\sqrt{\mu\varepsilon_o}\sqrt{1-(f_c/f)^2}} = \frac{c}{\sqrt{1-(f_c/f)^2}} \tag{10}$$

and a group velocity

$$v_g = \frac{c^2}{v_p} = c\sqrt{1-(f_c/f)^2} \tag{11}$$

These expressions will be recognized as those familiar in wave guide theory except for the definition of f_c.

APPENDIX II.

A. Power Amplifier Design

Tubes - 2 Eimac 4CN15 ceramic tetrodes operated in push-pull.

The published curves were revised for operation with 1000 volts on the screen grid by multiplying the plate and grid voltages by $\frac{1000}{250} = 4$. The increase in plate current was assumed to follow the three-halves power law[1] $I_p' \approx \left(\frac{1000}{250}\right)^{3/2} I_p$. The control grid current extrapolated to the higher positive grid region as well as possible from the published curves. The class 'C' design was carried out using the 15° increment Chaffee method[2].

Q point $E_p = 7000$ V $E_g = -300$ V

T point $E_p = 1600$ V $E_g = +100$

$E_{p\ max} = 5400$ V $E_{g\ max} = 400$ V

Point	$I_p(x\frac{1}{8})$ (amps)	I_g (amps)
A	1.3	2.4
B	1.25	2.1
C	1.05	.8
D	.52	0
E	.16	0
F	.05	0

Where A,B,C,D,E, and F are 15° increments on the load line.

---

[1] Terman, "Radio Engineers Handbook," McGraw-Hill Book Co., Inc., New York, N.Y., P. 298-300; 1943

[2] Albert, "Electronics and Electron devices," Macmillan Co., New York, N.Y., P. 289; 1956

For $E_{g_2} = 1000V$ $I_p' \approx I_p\left(\frac{1000}{250}\right)^{3/2} = 8I_p$, $V_p' = \left(\frac{1000}{250}\right)V_p = 4V_p$, $V_g' = 4V_g$, $I_g' \approx .8 + .0285\,(E_g' - 42)$ amps

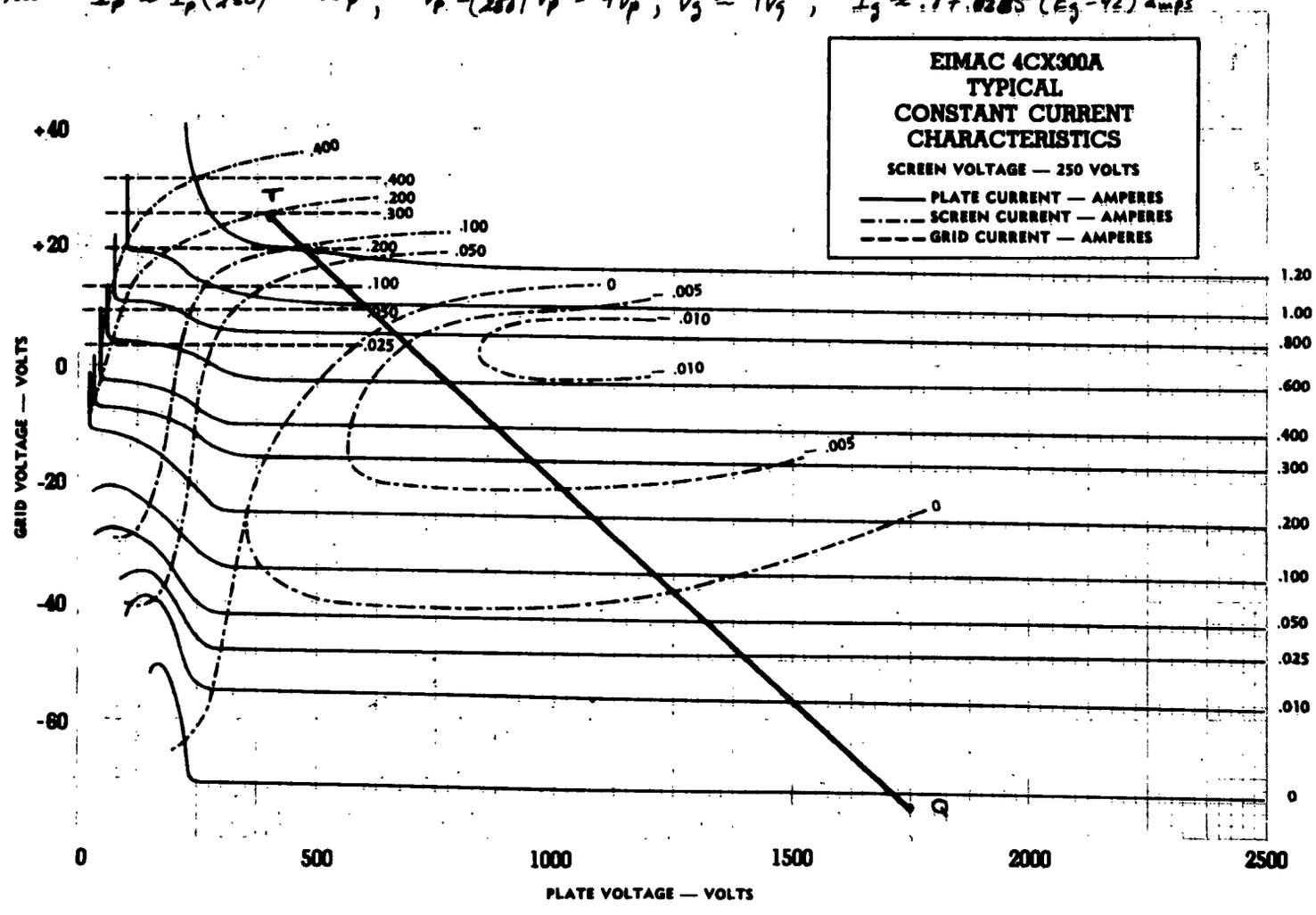

Printed in U.S.A. 8888

Peak Fundamental $I_{max} = \frac{1}{12}$ (A+1.93B+1.73C+1.41D+E+.52F)

$I_{pmax} = \frac{8}{12}$ (1.3+2.42+1.82+.73+.16+.03) = 4.32 amp

$I_{gmax} = \frac{1}{12}$ (2.4+4.05+1.38) = .65 amp

D.C. Component $I_{dc} = \frac{1}{12}$ (.5A +B+C+D+E+F)

$I_b = \frac{8}{12}$ (.65+1.25+1.05+.52+.16+.05) = 3.06 amp

Power Out $P_c = \frac{V_{max} I_{max}}{2} = \frac{4.32 \times 5400}{2}$ = 11.6 kw

Load Resistance $R_l = \frac{V_{max}}{I_{max}} = \frac{5400}{4.32}$ = 1250 Ω

Drive Power $P_{dr} = \frac{V_{g\ max} I_{g\ mas}}{2} = \frac{400x.65}{2}$ = 130 watts

D.C. Power $P_{in} = I_{dc} V_{dc}$ = 3.06x7000 = 21.4 kw

Efficiency = $\frac{P_o}{P_{in}} = \frac{11.6}{21.4}$ = 54%

B. Driver Design

Tube - Amperex 5894 dual tetrode, both halves operated in parallel.

The published characteristic curves were transformed for 600 volts screen grid potential in the same manner as part A.

Q point E_p = 1000 V E_g = -95 V

T point E_p = 200 V E_g = +12 V

$E_{p\ max}$ = 800 V $E_{g\ max}$ = 107 V

Point	I_p (amps.) ($\times \frac{1}{3.7}$)
A	.30
B	.29
C	.24
D	.16
E	.05
F	0

$$I_{p(max)} = \frac{3.7}{12} (.30+.56+.42+.22+.05) = .48 \text{ amp}$$

Power Out $= \frac{V_{max} I_{max}}{2} = \frac{800 \times .48}{2} = 192$ watts

Load Resistance $R_1 = \frac{V_{max}}{I_{max}} = \frac{800}{.48} = 1660\ \Omega$

For 2 tubes in parallel

$$P_o = 2 \times 192 = 384 \text{ watts}$$

$$R_1 = \frac{1660}{2} = 830 \text{ ohms}$$

BIBLIOGRAPHY

Millman and Taub, "Pulse and Digital Circuits," McGraw Hill Book Co., Inc., New York, New York, 1956.

Kraus, John D., "Antennas", McGraw Hill Book Co., Inc., New York, New York, 1950.

Ramo, Simon and Whinnery, John R., "Fields and Waves in Modern Radio", John Wiley and Sons, Inc., New York, New York, 1953.

Laudee, Davis, and Albrecht, "Electronic Designers Handbook," McGraw Hill Book Co., Inc., New York, New York, 1957

Martin, Thomas L., "Electronic Circuits", Prentice-Hall, Inc., Englewood Cliffs, 1956.

Kraus, John D., "Electromagnetics", McGraw Hill Book Co., New York, New York, 1953.